Supporting Information

A ligand-modulated photostable Mn(I)-carbonyl complex for preferential conversion of CO2 to CO in water

Chandan Das, Suchismita Ghosh, Rathindranath Biswas, Goutam K. Lahiri and Arnab Dutta

Table of contents:

Experimental Section:

1.1 Materials and Methods:

$Mn(CO)_5Br$, Bromopentacarbonylmanganese(I), (Alfa aeser reagent grade, ACS 98.0%), 2,6-di amino pyridine and 2-amino pyridine was purchased from Sigma-Aldrich India. Nitrosobenzene, tetrabutylammonium tetrafluoroborate were purchased from TCI India Pvt. Ltd. Acetone (HPLC and Spectroscopy), N, N-Dimethylformamide (HPLC and Spectroscopy), triethylamine (Dry, AR) and diethyl ether (AR), methanol (HPLC and gradient), chloroform (AR/ACS), triethanolamine (AR), hydrochloric acid (AR/ACS), sodium hydroxide (AR), sodium sulfate, anhydrous (AR/ACS), potassium chloride (AR), acetonitrile (HPLC and Gradient), phenol(AR/ACS), TFE,(trifluororthaol)(AR/ACS) and sodium chloride (AR) were purchased from Finar Chemicals Pvt. Ltd. India. All the analytical reagents were used as received without any further purification. Solvents are distilled using standard protocols. HPLC grade organic solvents and Millipore water (18.2 MΩ.cm resistivities at 298K) were used in all synthesis and chemical analyses. Glassware was oven dried before use. All the reactions were performed under air. Nuclear Magnetic Resonance (NMR) spectra were recorded at ~298K temperature using a Bruker Avance III Ascent FT spectrometer with working frequencies of 400 MHz for ^{1}H. NMR signals are reported in δ (ppm) units while employing the solvent signals of $CDCl_3$ (δ=7.3ppm) and $(CD_3)_2SO$ (δ=2.50 ppm) as internal standard along with TMS (δ=0 ppm). The optical spectra were recorded on a PerkinElmer Lambda 1050 spectrometers using 1 cm path length in 2 mL volume Sterna make quartz cuvette. The FTIR spectra of samples were recorded in the OTTLE cell by dissolving in DMF. HRMS of the samples was recorded with a Bruker maXis impact in positive mode. Cyclic voltammetry (CV) experiments were carried out at room temperature using Metrohm Autolab PGSTAT 204 potentiostat. All measurement was carried out in dry DMF using TBAF as a supporting electrolyte. A standard three electrode system under Ar atmosphere was used with a 1 mm glassy carbon disc as a working electrode, Ag as a reference electrode connected by vycor tip and a platinum wire as counter electrode. All potentials are reported versus ferrocene ($Fc^{0/+}$) couple for organic medium. Optical spectroelectrochemistry experiments were performed at room temperature in DMF solution using Ocean Optics spectrophotometer with 240.00 ms integration time and near 10 average scans. 2 ml of sample was placed in a 3.5 ml quartz cuvette (1 cm path length) placed in an external sample holder connected to light source and detector via optical fibres. System was further connected to a Metrohm Autolab PGSTAT204 using a 3 mm glassy carbon rod as working electrode, Pt wire as counter electrode, and Ag as a reference electrode with

continuous Ar and CO_2 pressure respectively. Infrared spectroelectrochemistry experiments were performed employing an optically transparent thin–layer electrode (OTTLE) cell, equipped with Pt mesh as working electrode, Pt microwire as counter electrode, and Ag microwire as a pseudo–reference electrode. The electrodes of this cell were simultaneously connected to a Metrohm Autolab PGSTAT204 for electrochemical measurements.

1.2 Synthetic Procedure:

1.2.1 [2,6-diphenyl(di-azo)] pyridine (L1):

The ligand [2,6-diphenyl(di-azo)] pyridine (**L1**) was synthesized by slight modification of previously reported synthesis of the ligand, phenyl azo pyridine by Lahiri and co-workers.[1] 0.5 g (4.5mmol) of 2,6-di amino pyridine was dissolved into 20 mL of tert-butanol solvent in a 200 mL RB. To this solution, 50% aqueous NaOH was added and while stirring at 50˚C for 1.5 h. After that, 0.98 g nitrosobenzene (9 mmol, 2 equivalent) was added into the solution. Then the whole reaction mixture was refluxed at 100°C for 24 h. After workup and through column chromatography we purified and synthesized the ligand. The ligand **(L1)** is confirmed by ^{1}H (Figure S1a), ^{13}C (Figure S2) NMR and HRMS.

1.2.2 3,5-bis(2-pyridyl)-4-amino-1,2,4-triazole (L2):

The ligand 3,5-bis(2-pyridyl)-4-amino-1,2,4-triazole pyridine (**L2**) was synthesized by modifying the previously reported procedure.[2] This ligand was prepared through two step process. For first step 3,6-bis(2-pyridyl)-1,2-dihydro1,2,4,5-tetrazine preparation: At first, mixture of 2-cyanopyridine and hydrazine dihydrochloride soluble in ethylene glycol in a two neck RB and then heated with 50°C for 30 minutes. Then excess amount of hydrazine hydrate was added under N_2 atmosphere. After that this whole mixture was further kept under microwave irradiation for 18hrs. Thus 3,6-bis(2-pyridyl)-1,2-dihydro1,2,4,5-tetrazine ligand was prepared. For second step: 3,5- bis(2-pyridyl)-4-amino-1,2,4-triazole was prepared through arrangement of 3,6-bis(2-pyridyl)-1,2-dihydro1,2,4,5-tetrazine ligand by treatments of dilute hydrochloric acid at 80°C. Then the ligand was purified by column chromatography and confirmed by ^{1}H, ^{13}C NMR & HRMS.

1.2.3 $Mn(CO)_3Br$(L1): [1]

574 mg (2.0 mol) of [2,6-diphenyl(di-azo)] pyridine was dissolved in 30 ml methanol to obtain a reddish colour solution. This methanolic solution was added dropwise to an orange colour solution of a 50 ml DCM containing 550.0 mg (2.0 mol) of $Mn(CO)_5Br$. The reaction mixture was stirred overnight at room temperature until a deep brown solution was obtained in

a dark condition. It was followed by the addition of cold (253K) 200 ml of di-ethyl ether to obtain a brown colour precipitate. The precipitate was kept in freezer for 5 hrs to get settled down, the precipitate was collected with Whatman filter paper and dried in vacuum. The brown ppt was dissolved in methanol/DCM (1:1) for crystallization. Yellowish crystals appeared after 1 week which was further dried under vacuum. Yield: 1.7 g (71.3% with respect to Ligand). HRMS (ESI, +ve mode, ACN) m/z for (M^+) [$C_{20}H_{13}MnN_5O_3$]: Calculated: 426.039, Experimental: 426.032. Optical spectral signals recorded in DMF.

1.2.4 $MnBr_2$(L1): [1a]

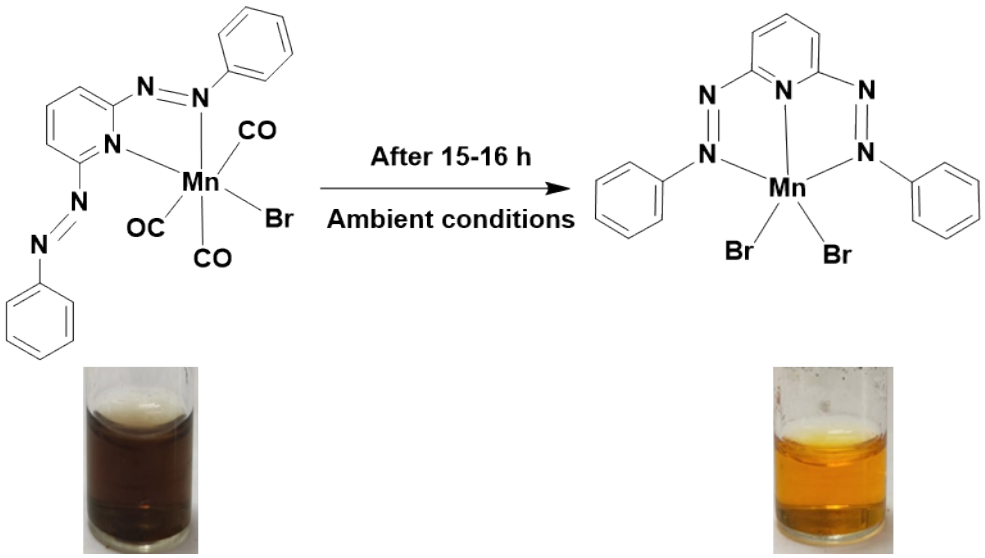

To check the stability of the complex **1,** we prepared a DMF solution of the complex and kept at ambient condition. We noticed the gradual change of color of the solution in 6-7 h from dark to light brown. Over time the color kept changing, and after 19 to 20 h a brownish yellow solution was obtained. Then the solution was kept for crystallization and after slow evaporation in air we got reddish brown crystals. HRMS (ESI, +ve mode, ACN) m/z for (M^+) [$C_{17}H_{13}BrMnN_5$]: Calculated: 420.97, Experimental: 420.95. Optical spectral studies were performed in DMF.

1.2.5 $Mn(CO)_3Br(L2)$: [2]

478 mg (2.0 mol) of 3,5-bis(2-pyridyl)-4-amino-1,2,4-triazole pyridine was dissolved in 20 ml methanol to obtain a colourless solution. This methanolic solution was added dropwise to an orange colour solution of a 50 ml DCM containing 550.0 mg (2.0 mol) of $Mn(CO)_5Br$. The reaction mixture was stirred overnight at room temperature until a deep brown solution was obtained in a dark condition. It was followed by the addition of cold (253K) 200 ml of di-ethyl ether to obtain a brown colour precipitate. The precipitate was allowed to keep in freeze for 5-7 hrs to get settled down, the precipitate was collected with Whatman filter paper and dried in vacuum. The brown colour ppt was dissolved in methanol/DCM (1:1) for crystallization. Yellowish colour crystals appeared after 1 week that was further dried under vacuum. Yield: 1.0 g (52.3% with respect to Ligand). HRMS (ESI, +ve mode, ACN) m/z for (M^+) [$C_{15}H_{10}MnN_6O_3.CH_3CN$]: Calculated: 418.04, Experimental: 418.04. Optical spectral signals recorded in DMF.

1.3 Cyclic voltammetry study in organic solvent:

The cyclic voltammetry experiment was primarily executed in an organic medium (DMF) and in water (H_2O) at a room temperature. The analyte concentration was maintained at 1 mM in all the cases unless mentioned otherwise. The 0.1 M tetrabutylammonium tetrafluoroborate (TBAF, $nBu_4N^+BF_4^-$) was employed as the supporting electrolyte for DMF and 0.1 M $KHCO_3$ for aqueous media. The cyclic voltammograms were recorded using a typical three-electrode assembly, wherein a 1 mm diameter glassy carbon disc utilized as working electrode, Pt-wire as counter electrode, and Ag/AgCl (saturated KCl) as reference electrodes. Hence, all the potential values in organic media in this study were reported against ferrocene couples ($Fc^{+/0}$).

1.4 Spectroelectrochemistry (Optical):

Optical spectroelectrochemistry experiments were performed via an Ocean Optics spectrophotometer in tandem with a Metrohm Autolab PGSTAT204 potentiostat. The sample was placed in a 3.5 ml quartz cuvette (1 cm path length) fixed in an external sample holder and connected to a light source and a detector via optical fibres. The cuvette was also fitted with a 3 mm glassy carbon rod working electrode, a Pt wire counter electrode, and a silver wire as reference electrode. A controlled potential electrolysis (CPE) experiment was performed with the use of the potentiostat, while the respective changes in the optical spectrum were monitored with the spectrophotometer.

1.5 Spectroelectrochemistry (FTIR):

An optically transparent thin–layer electrode (OTTLE) cell, equipped with a Pt mesh working electrode, a Pt microwire counter electrode, and Ag microwire pseudo–reference electrodes were employed for this study along with a Metrohm Autolab PGSTAT204. All the FTIR spectra were measured using a Perkin–Elmer FTIR spectrometer set in absorbance mode. All the measurements were carried out at room temperature with ~30mM complex concentration. Data was also recorded for a CO_2-saturated blank DMF solution and subtracted from all the experimental data collected under the CO_2 atmosphere.

1.6 Single crystal X-ray diffraction study:

Crystals of the complex were grown from methanol/hexane layering by a solvent evaporation method. A suitable brown crystal for the complex was selected and mounted on a cryo-loop using cryoprotectant paratone oil. The single-crystal diffraction data for the crystal was collected at 150K in a Bruker D8 Quest diffractometer equipped with an Incoatec Microfocus Source (IμS 3.0 Mo Kα, λ = 0.71073 Å) and a PHOTON II detector. X-ray diffraction intensities were collected, integrated, and scaled with APEX4 software. Empirical absorption correction was applied to the data by employing the multi-scan method with SADABS programming.[3] Structure was solved by intrinsic phasing with SHELXT[4] and, refined by full-matrix least-square methods on F^2 using SHELXL using the ShelXl along with Olex2 interface.[5,6] All non-hydrogen atoms were refined with anisotropic displacement parameters. The hydrogen atoms were introduced at a calculated positions and were treated as riding atoms with an isotropic displacement parameter, C-H = 0.93-0.98 A° with Uiso(H) = 1.5UeqI for methyl groups, Uiso(H) = 1.2Ueq(C, N) for all other C—H and N—H bonds and O—H = 0.82 A˚ [Uiso(H) = 1.5Ueq(O)]. Mercury, PLATON and publCIF was used for molecular graphics, validation and to prepare material for publication.[4,7,8] Details of crystal data collections and data refinement parameters are given in **Table S1**. The complete crystallographic information file (CIF) for the complex was deposited in Cambridge crystallographic data centre (**CCDC** no. 2063724 (**1**), 2060736 (**2**), 2236211 (**3**)).

1.7 Rinse Test:

A rinse test for complexes has been carried out in an organic medium (DMF) to probe the homogeneous or heterogeneous nature of the catalysis. For this purpose, we have executed three consecutive runs as follows. A complete CV was recorded for the complexes in the corresponding organic medium under the CO_2 atmosphere in the first run. Then the working electrode was thoroughly rinsed with water. Then this electrode was properly polished with 0.25 μm alumina powder. Afterward, a second run was performed with the same complex solution with the cleaned working electrode. However, this second run was stopped at the potential where the maximum CO_2 reduction signal was observed. Then the working electrode was only rinsed (without any polishing) with water, and a third cyclic voltammogram was recorded in a different solution that contained only blank DMF and the electrolyte but no complex. This third scan was initiated again from the maximum catalytic response potential observed for CO_2 reduction. The absence of any significant catalytic response in the third scan in the reduction direction validates the homogeneous CO_2 reduction mechanism. Like, under DMF, to prove homogeneous catalysis in water, same experiment was done in water medium.

1.8 Gas chromatography analysis:

The amount of CO_2/CO evolved during catalysis were quantified by using Dhruva CIC gas chromatography (GC) instrument equipped with TCD detector having a 5Å molecular sieve/Porapak 13X column using Ar as carrier gas.

1.9 Calculation of catalytic rate:

Catalytic rate of the complexes was measured from equation S1:

$$\frac{i_{cat}}{i_p} = \frac{n_{cat}}{0.4463 \cdot n_p}\sqrt{\frac{RTk_{obs}}{F\nu}} \qquad \textbf{(Equation S1)}$$

where, i_{cat} = catalytic current, i_p = stoichiometric current, n_{cat} = number of electrons involved in the catalytic process, n_p = number of electrons involved in the stoichiometric process (= 1), R = universal gas constant, T = temperature in K, F = 1 Faraday, and ν = scan rate.

1.10 Bulk or Control Potential Experiment:

Bulk Electrolysis (BE) or control potential experiment (CPE) was performed in an air-tight 95 ml four neck glass vessel. Three of these outlets were fitted with various electrodes; 2 cm x 1 cm vitreous carbon as a working electrode; 23 cm coiled platinum wire as a counter electrode, and Ag wire as a reference electrode. The last outlet was closed by a B-14/20 suba® seal rubber

septum, which was used for purging CO_2 or CO or Ar (for 30 minutes) before the experiments and for headspace gas collection. During an experiment, 14 ml of 1 mM complexes were added to the vessel, all electrodes (along with a magnetic bead) were inserted along with a B-14/20 rubber septum cap (in a gas-tight manner). Then, the chrono-coulometric experiment was started at corresponding catalytic potentials in both organic and aqueous media. The reaction solution was continuously stirred during the experiment. Headspace gas was collected by a GASTIGHT® PTFE leur-lock 1000 series (1001TLL) 1 ml 8 Hamilton® syringe after certain time intervals, and it was analyzed via gas chromatography (GC) instrument on TCD/FID mode.

2. Results

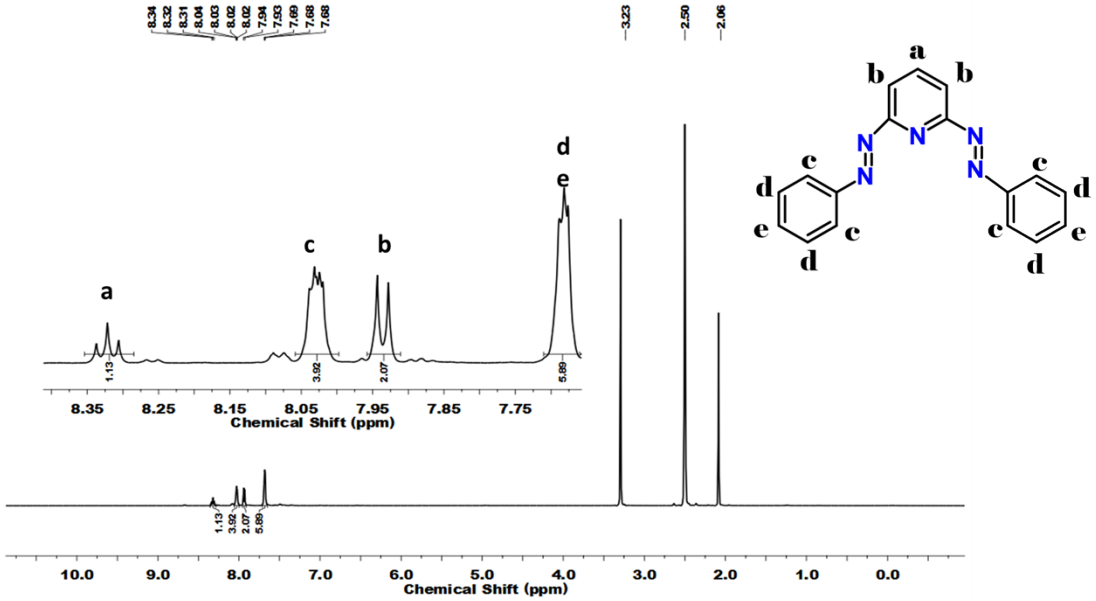

Figure S1. ^{1}H and NMR of L1

^{1}H NMR spectrum of ligand L1 recorded in d^{6}-DMSO at 298 K. The inset highlights the NMR signal distribution in δ 7.0-8.5 ppm.

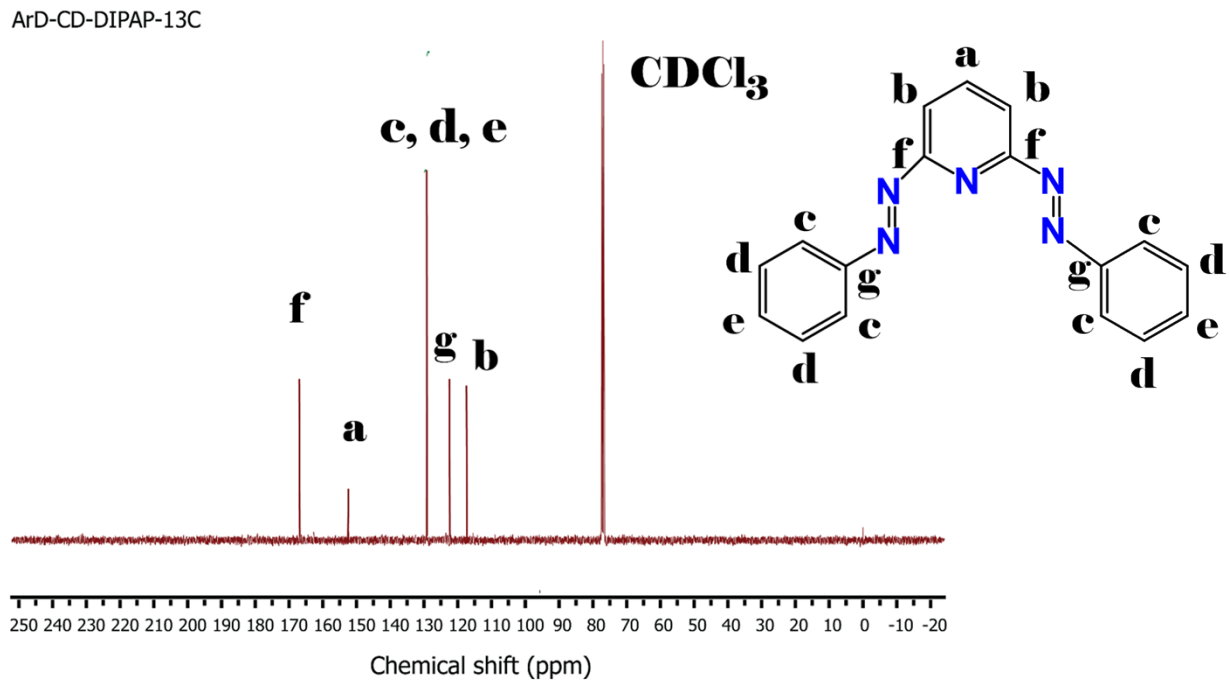

Figure S2. ^{13}C NMR of L1

^{13}C NMR spectrum of ligand L1 recorded in $CDCl_3$ at 298 K.

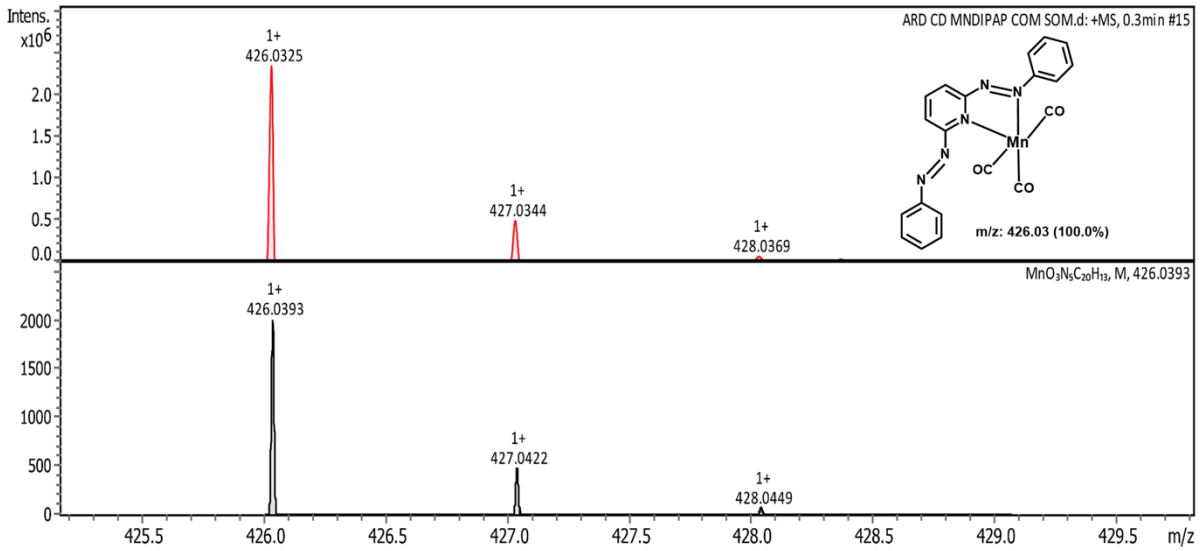

Figure S3. ESI-MS of 1.

Spectra recorded in CH_3CN at 298 K. Simulated (red trace), experimental (black) data are stacked for comparison.

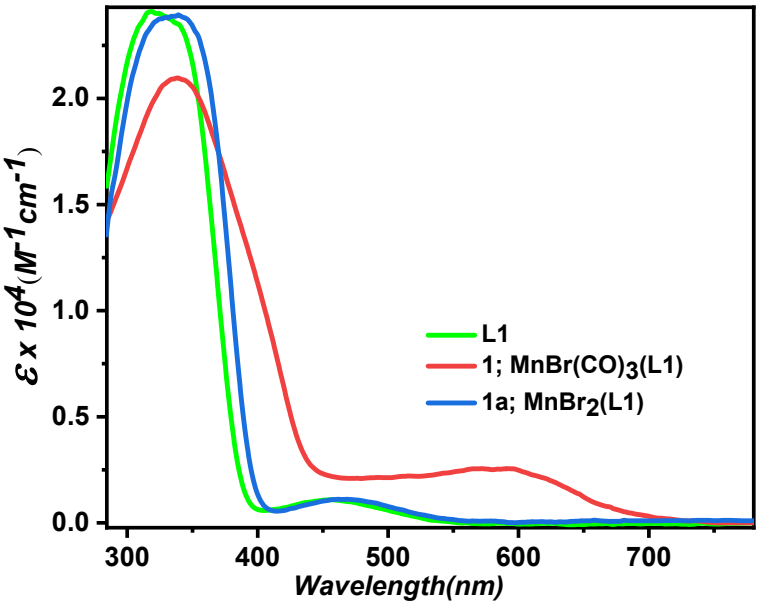

Figure S4. UV-Vis Spectra L1, 1 and 1a

Optical spectra data for the complexes 1, 1a and ligand L1 in DMF. Comparative spectra of L1 (green trace), 1 (red trace) and 1a (blue trace). All the spectra were recorded at room temperature scanning in the 300-800 nm range.

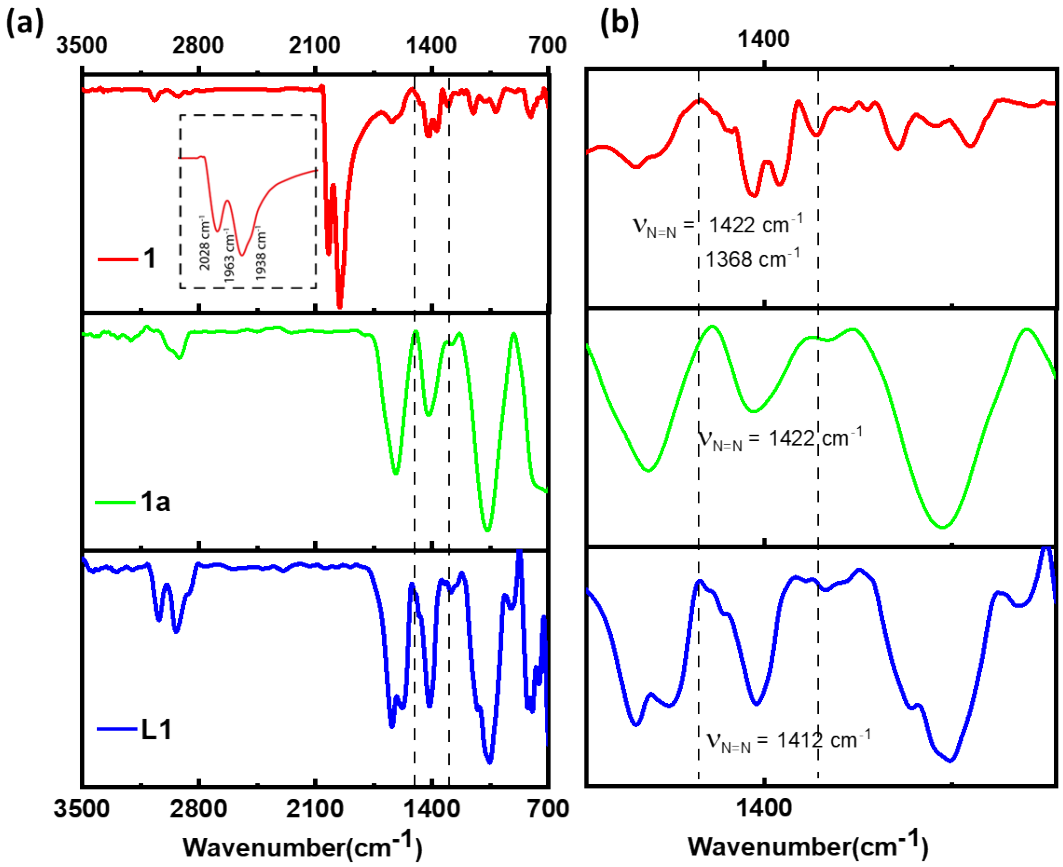

Figure S5. FT-IR Spectra of 1, 1a and L1

FTIR spectrum comparison between: (a) 1 (red trace), 1a (green trace) and L1 (blue trace). Inset highlights the region between 2100-1900 cm^{-1} highlighting CO stretching bands ν_{sym} = 2028 cm^{-1}, ν_{asym} = 1963 cm^{-1} and 1938 cm^{-1}; (b) Signal distribution between 1700-860 cm^{-1} to highlight $\nu_{N=N}$ stretching frequencies. Spectrum were recorded in % transmittance mode at room temperature using solid KBr pellet from 4000-400 cm^{-1} range.

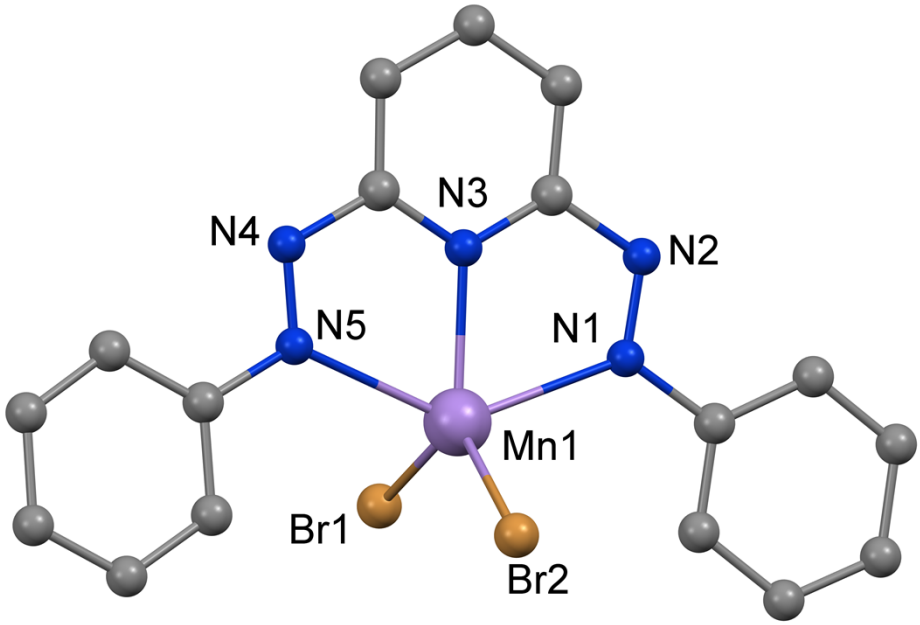

Figure S6. SCXRD structure of 1a.

C, N, Br, and Mn atoms are displayed as grey, blue, brown and purple spheres, respectively. The hydrogen atoms are omitted for clarity. CCDC 2060736

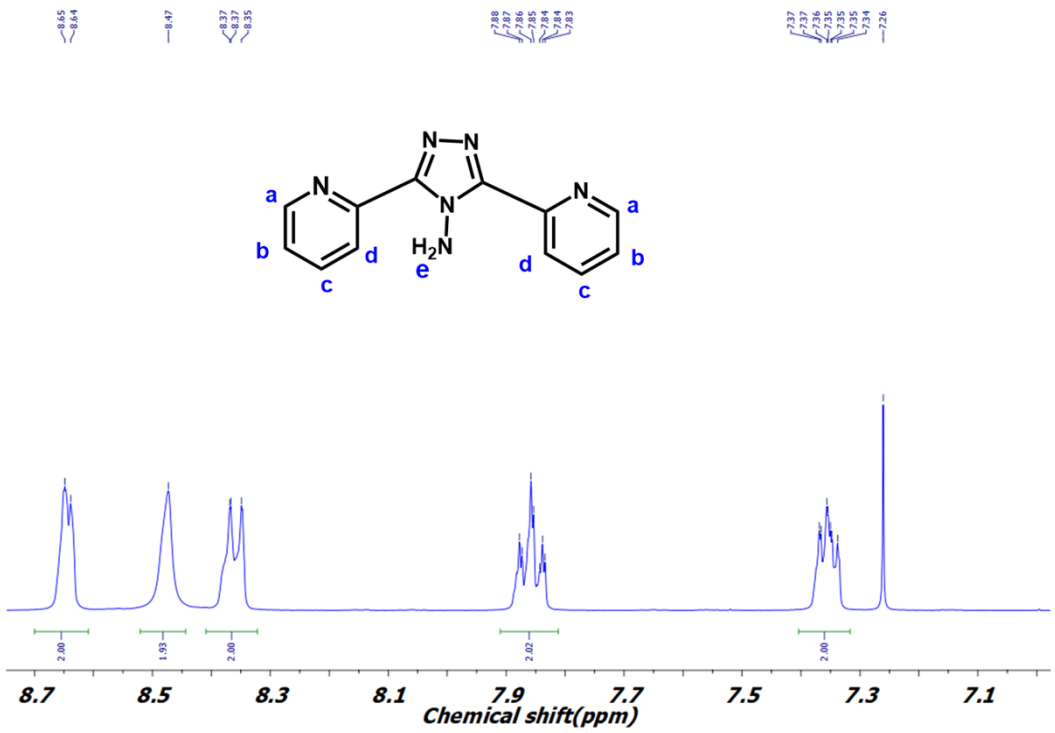

Figure S 7 ^{1}H NMR spectrum of L2

^{1}H NMR spectrum of ligand L2 recorded in $CDCl_3$ at 298 K.

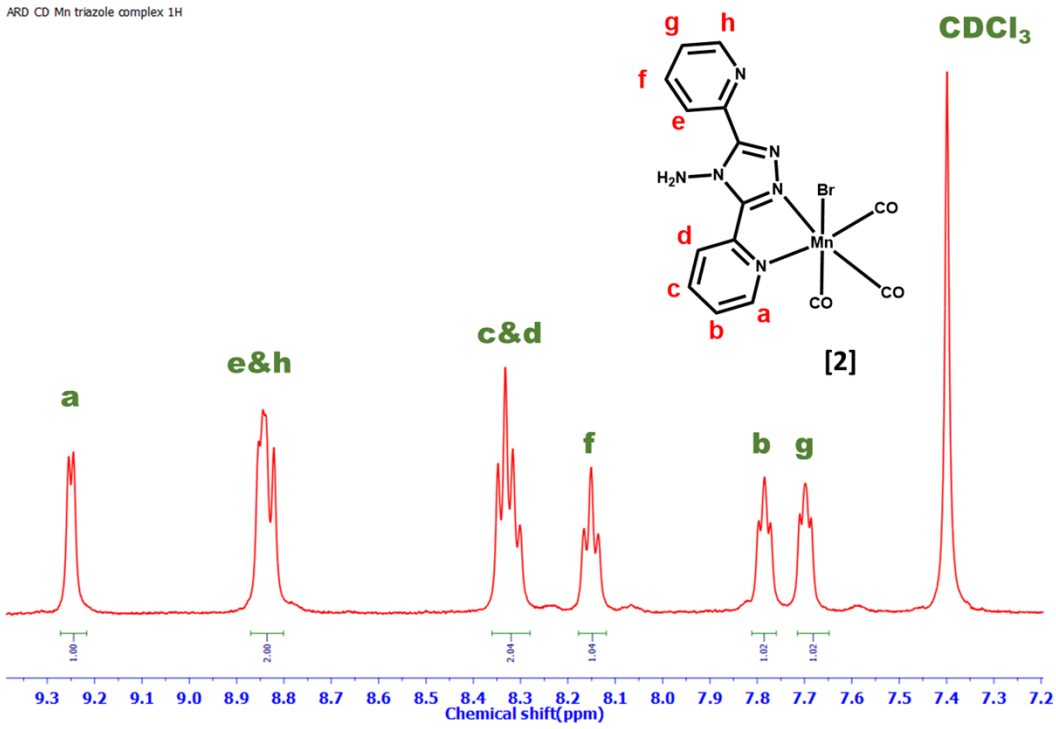

Figure S 8 ^{1}H NMR of 2

^{1}H NMR spectrum of complex **[2]** recorded in $CDCl_3$ at 298 K.

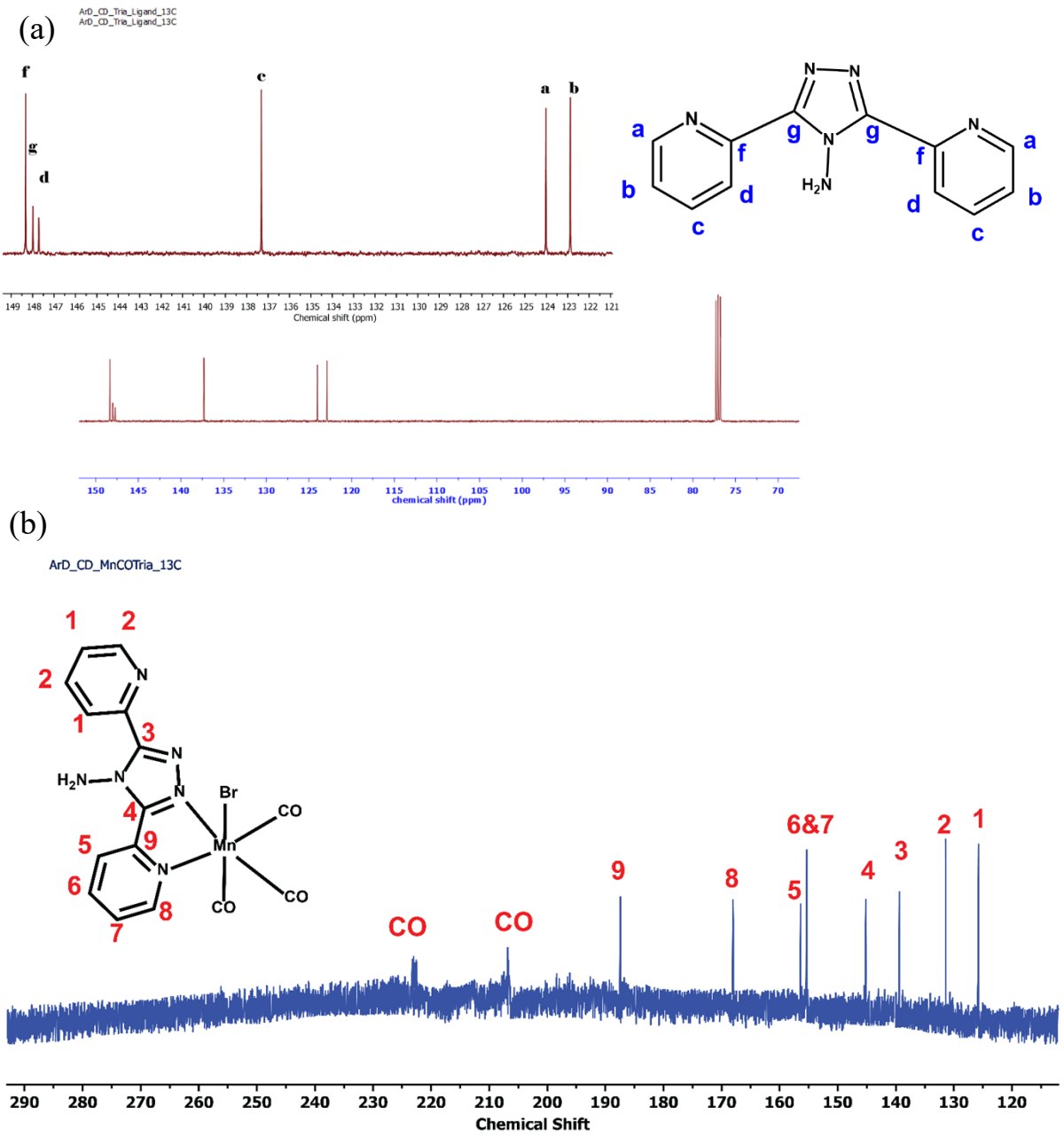

Figure S 9 ^{13}C NMR of L2 and 2

(a) ^{13}C NMR spectrum of ligand L2 recorded in $CDCl_3$ at 298 K. The inset highlights the NMR signal distribution in δ 120-150 ppm. (b) ^{13}C NMR spectrum of complex **[2]** recorded in $CDCl_3$ at 298 K

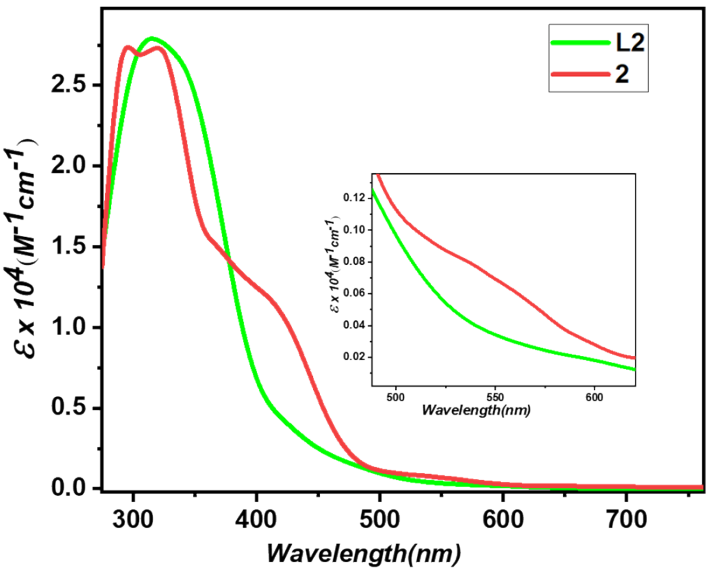

Figure S 10 UV-Vis Spectra of L2 and 2

Optical spectra data for ligand L2 and complex 2 in DMF. Comparative spectra of L2 (green trace) and 2 (red trace). The inset highlights the d-d band at 550 nm. All the spectra were recorded at room temperature scanning in the 300-800 nm range.

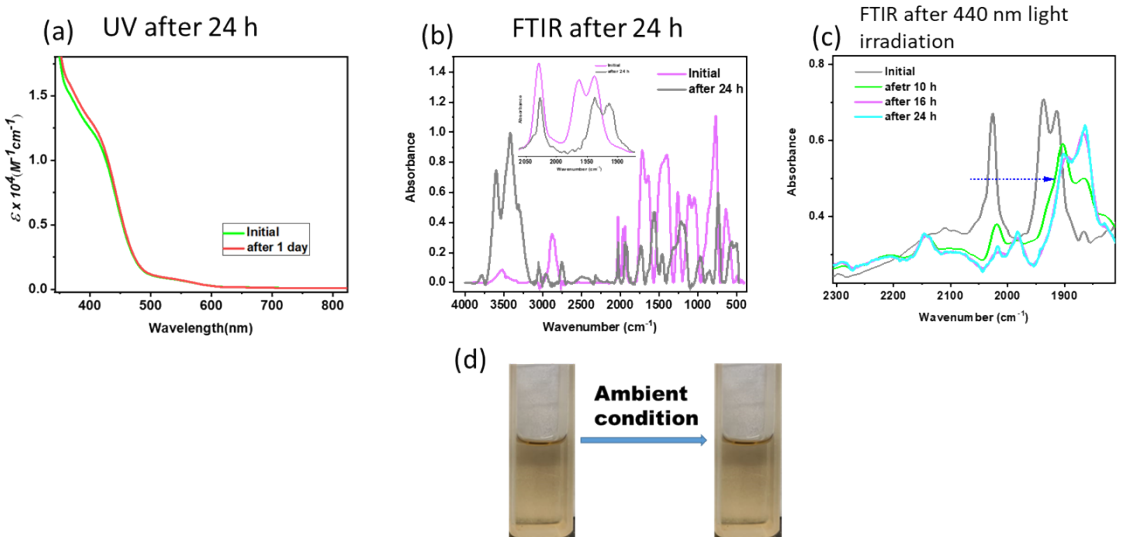

Figure S 11 Stability monitoring of 2

(a) Optical spectra data for the complex 2 recorded in DMF at room temperature in the scanning range of 300-800 nm. (b) Solution state FT-IT spectra of 2 recorded in DMF at room temperature. Comparative spectra of freshly prepared complex (green trace in UV and pink trace in FT-IR) and the spectra after one day (red trace for UV and grey trace for FT-IR) to check for stability. (c) Changes in

FT-IR after irradiation with 440 nm light source for 10 h (green trace), 16 h (pink trace) and 24 h (cyan trace). (d) Snapshots of the cuvette containing the DMF solution of freshly prepared metal complex and the same solution after one day. No visible colour change was observed.

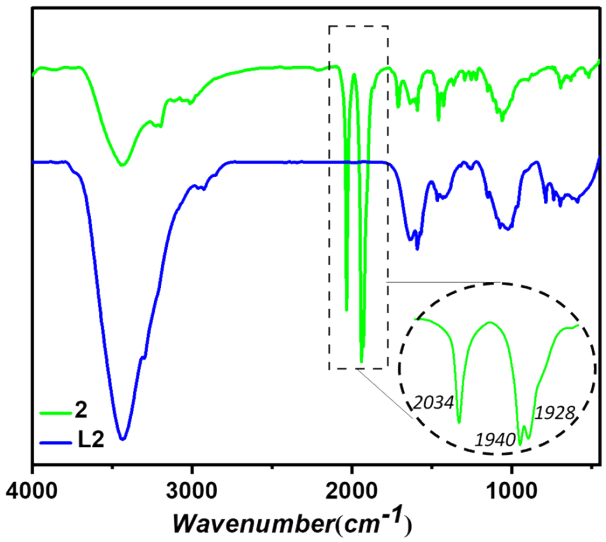

Figure S 12 FT-IR Spectra of L2 and 2

FTIR spectrum comparison between 2 (green trace) and L2 (blue trace); Inset shows signal distribution between 2100-1850 cm^{-1} to highlight ν_{CO} stretching frequencies. Spectrum were recorded in % transmittance mode at room temperature using solid KBr pellet from 4000-450 cm^{-1} range.

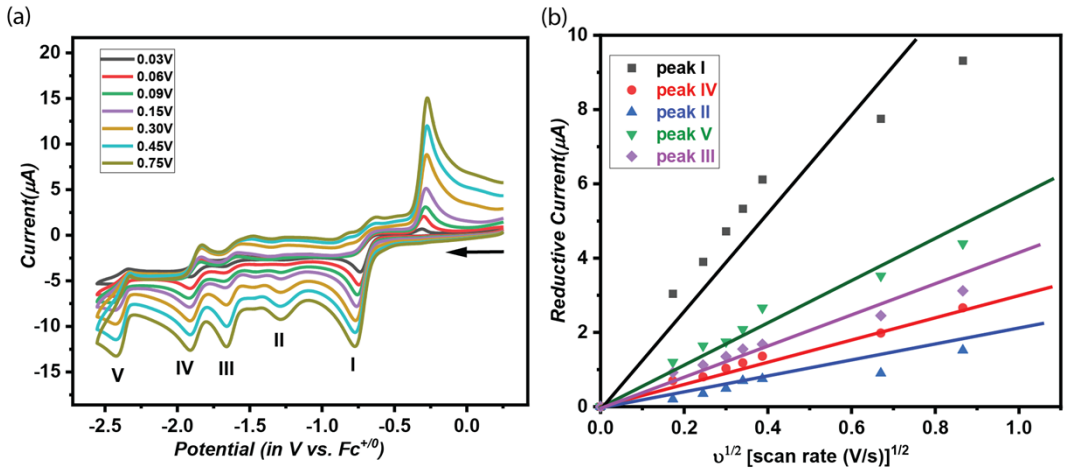

Figure S 13 CV of 1 at different scan rates under Ar

Cyclic Voltammetry (CV) study in Ar atmosphere for C1 complex; (a) CV with different scan rate (0.03 V/sec to 0.09 V/sec); (b) $\nu^{1/2}$ vs reductive current plots of each peak. A 1mM catalyst in 0.1 M TBAF

was used with glassy carbon working electrode, Pt counter electrode, and Ag/AgCl reference electrode in DMF at 289K temperature. Arrow describes origin and direction of scan.

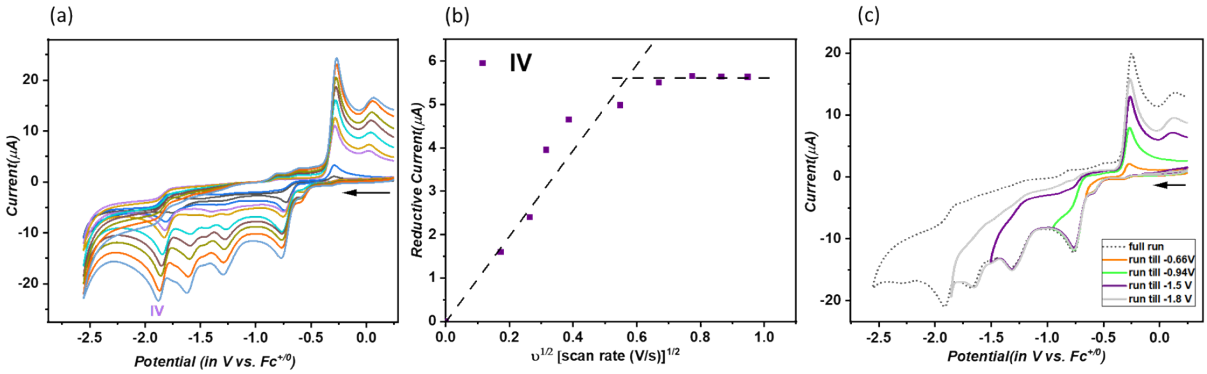

Figure S 14 CV studies of 1 at different scan rates under CO_2

(a) The cyclic voltammograms recorded for 1 under CO_2 atmosphere at variable scan rates (0.03 V/sec to 0.9 V/sec). (b) The trend of change in reduction current vs. square root of scan rate ($\nu^{1/2}$) for the CO_2 reduction signal at -1.9 V (IV). (c) Potential sweeping from 0.2 V to -2.5 V at scan rate 100 mV/sec. A 1mM catalyst in 0.1 M TBAF was used with glassy carbon working electrode, Pt counter electrode, and Ag/AgCl reference electrode in DMF at 289K temperature. The horizontal arrow describes the initial scan direction.

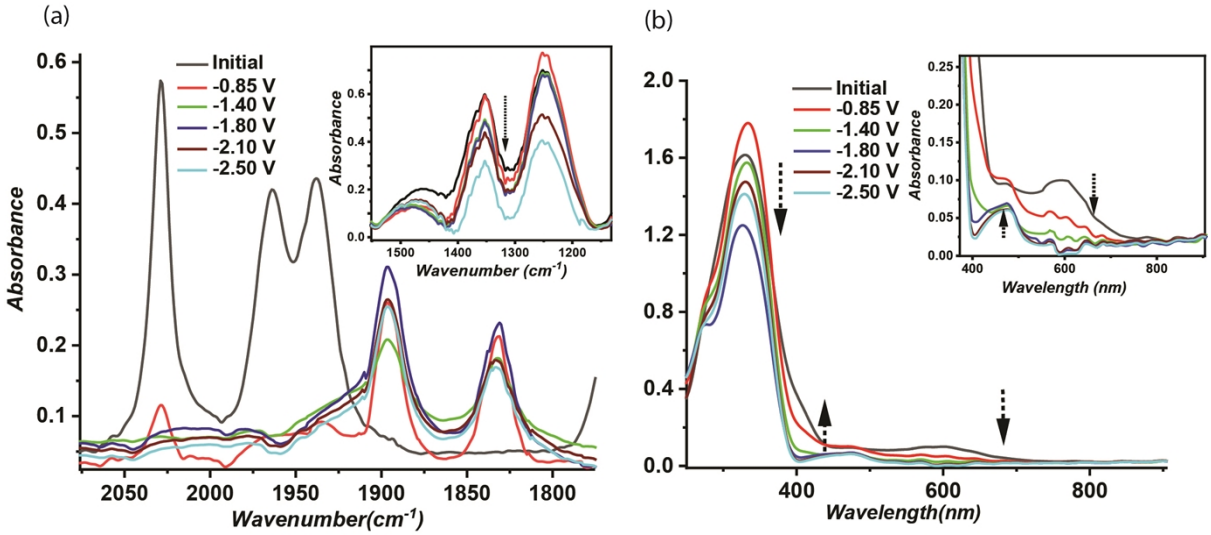

Figure S 15 Spectroelectrochemical analysis for 1 under Ar.

(a) SEC-IR showing changes in CO stretching bands and inset shows changes in azo band frequency. (b) SEC-optical shows changes in π-π*(375 nm)[9] and d-d transition (590 nm)[10,11] and MLCT bands (450 nm).[9] Inset highlights the 400-800 nm range. All data were recorded in DMF at 298K temperature.

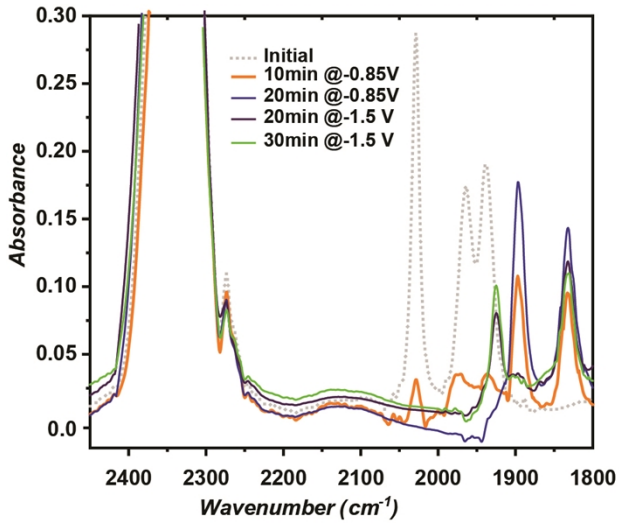

Figure S 16 IR-SEC analysis for 1 under CO_2.

Changes in IR-SEC at applying constant potentials of -0.85 V and -1.5 V. All data were recorded in DMF at 298K temperature.

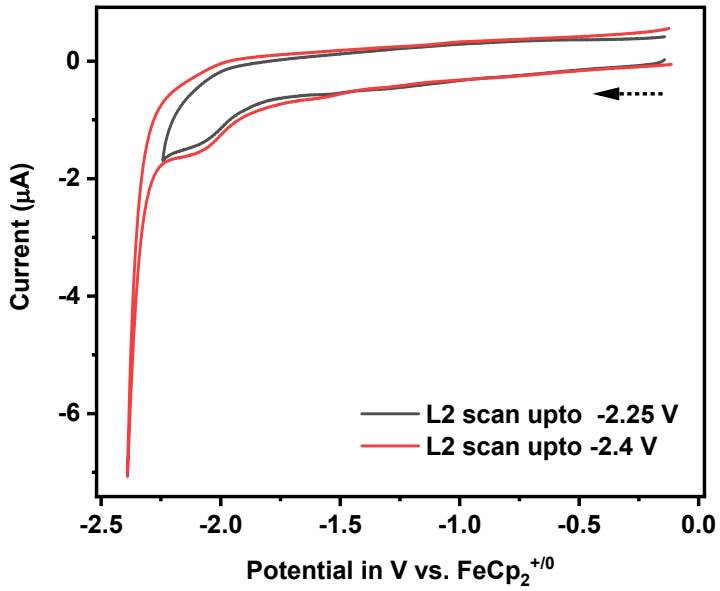

Figure S 17 CV studies of L2 under Ar

Cyclic Voltammetry (CV) study in Ar atmosphere for L2 in the potential range of 0.25 to -2.25 V (black trace) and 0.25 to -2.4 V (red trace) at a scan rate of 0.1 V/sec. A 1mM compound in 0.1 M TBAF was used with glassy carbon working electrode, Pt counter electrode, and Ag/AgCl reference electrode in DMF at 289K temperature. Arrow describes origin and direction of scan.

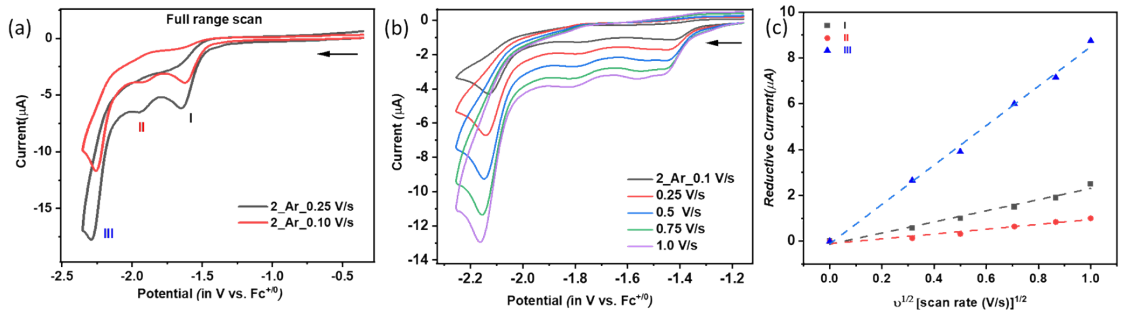

Figure S 18 CV studies of 2 at different scan rates under Ar

Cyclic Voltammetry (CV) study in Ar atmosphere for complex 2; (a) CV at in the potential range of -0.5 V to -2.5 V at scan rates 0.25 V/sec and 0.1 V/sec. (b) CV at different scan rate (0.1 V/sec to 1 V/sec); (b) $\nu^{1/2}$ vs reductive current plots of each peak. A 1mM catalyst in 0.1 M TBAF was used with glassy carbon working electrode, Pt counter electrode, and Ag/AgCl reference electrode in DMF at 289K temperature. Arrow describes origin and direction of scan.

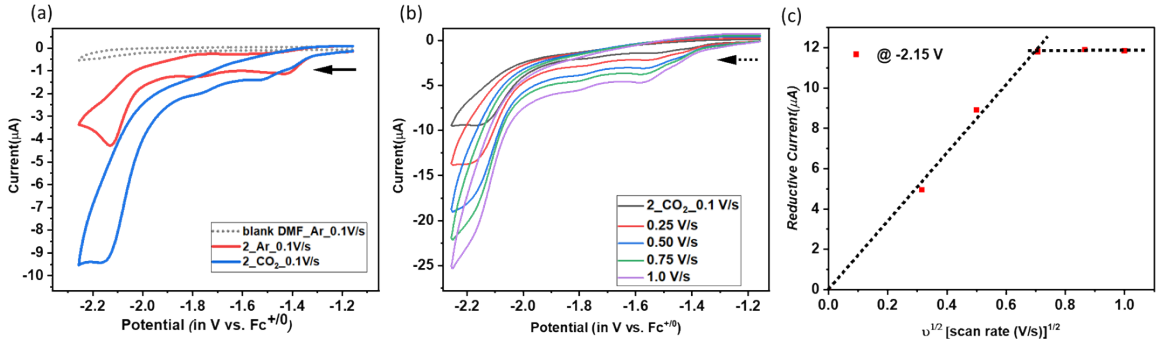

Figure S 19 CV studies of 2 at different scan rates under CO_2

(a) The cyclic voltammograms recorded for DMF (dotted trace), 2 under Ar (red trace) and 2 under CO_2 (blue trace) at 0.1 V/sec scan rate. (b) CV of 2 under CO_2 at variable scan rates (0.1 to 1 V/sec). (c) The trend of change in reduction current vs. square root of scan rate ($\nu^{1/2}$) for the CO_2 reduction signal at -2.15 V. A 1mM catalyst in 0.1 M TBAF was used with glassy carbon working electrode, Pt counter electrode, and Ag/AgCl reference electrode in DMF at 289K temperature. The horizontal arrow describes the initial scan direction.

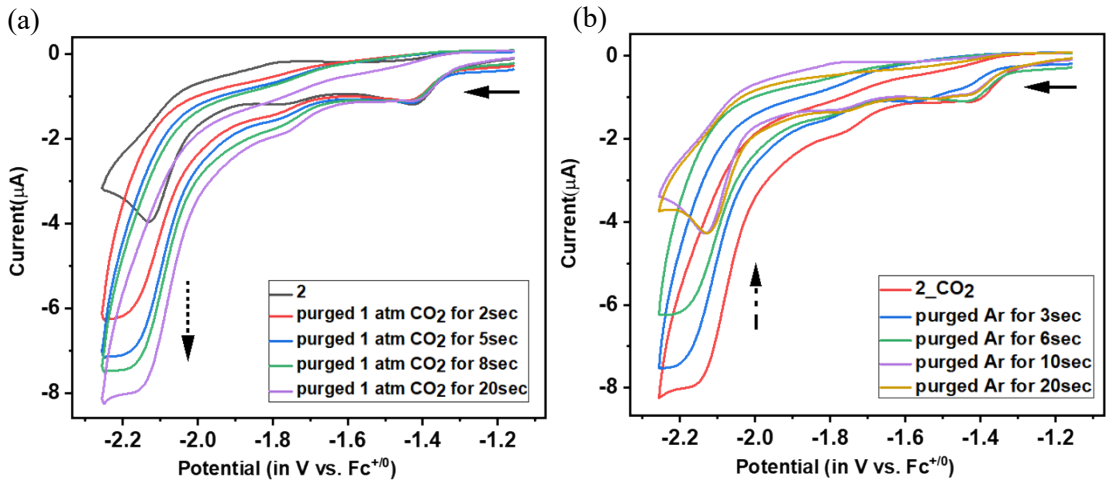

Figure S 20 Change in CV profile of 2 under gradual addition of CO_2 and Ar

(a) CV recorded after purging CO_2 gradually at different time intervals and, (b) purging Ar gradually to the saturated CO_2 solution of 2. All data were recorded in DMF (with externally added 100 µL water) at 298K temperature at 0.1 V/sec. A 1mM catalyst in 0.1 M TBAF was used with glassy carbon working electrode, Pt counter electrode, and Ag/AgCl reference electrode. The horizontal arrow describes the initial scan direction.

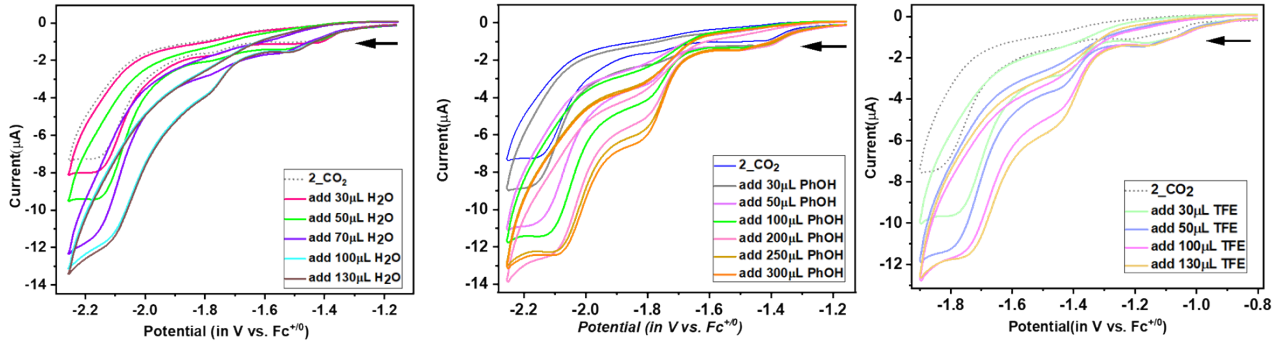

Figure S 21 Changes in CV profile of 2 under CO_2 in the presence of various external proton sources

Changes in CV in the presence of varying amounts of (a) Water, (b) Phenol and (c) Trifluoroethanol as proton sources. A 1mM catalyst in 0.1 M TBAF was used with glassy carbon working electrode, Pt counter electrode, and Ag/AgCl reference electrode in DMF at 289K temperature at 0.1 V/sec. The horizontal arrow describes the initial scan direction.

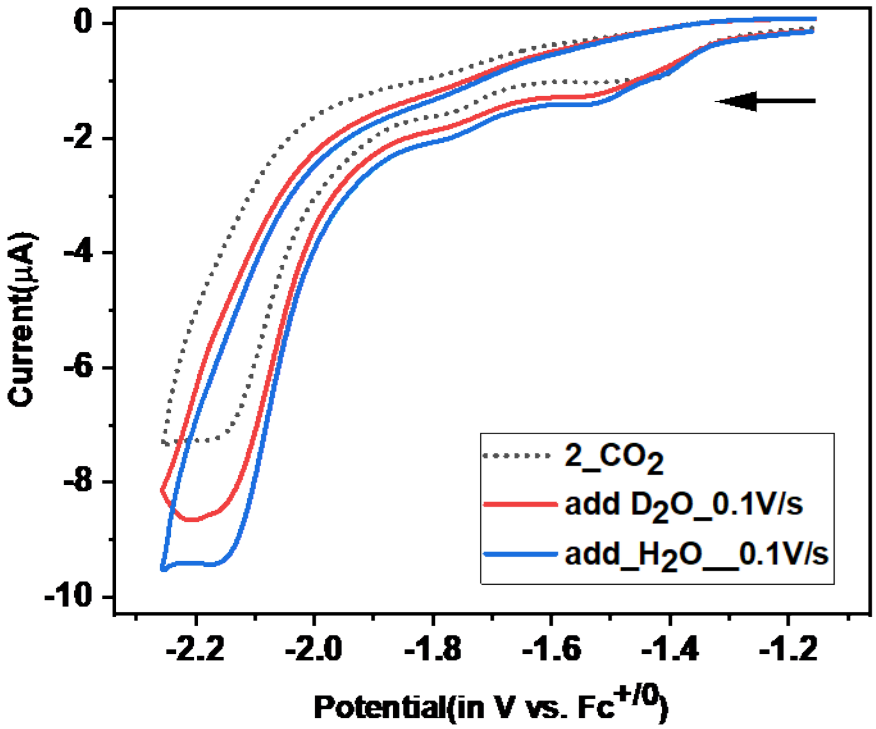

Figure S 22 Kinetic isotopic studies of 2

The Cyclic Voltammograms of (a) 2 under 1 atm CO_2 (dotted trace), (b) 2 under CO_2 after addition of D_2O (red trace) and (c) 2 under CO_2 after addition of H_2O (blue trace). All data were recorded in DMF at 298K temperature at 0.1 V/sec. The horizontal arrow describes the initial scan direction.

Calculated kinetic isotope effect (KIE) $K_H/K_D = 2.08$; K_H & K_D are the rate constants for the catalytic reactions using H_2O and D_2O respectively.

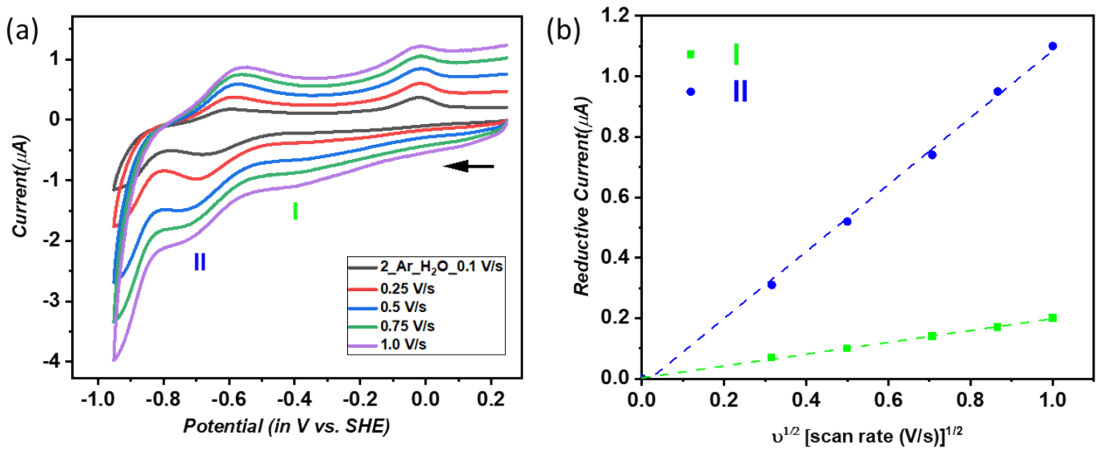

Figure S 23 CV studies of 2 under Ar in aqueous medium

Cyclic Voltammetry (CV) study in Ar atmosphere for complex 2; (a) CV at different scan rate (0.1 V/sec to 1 V/sec); (b) $v^{1/2}$ vs reductive current plots of each peak. A 1mM catalyst in 0.1 M $KHCO_3$ was used with glassy carbon working electrode, Pt counter electrode, and Ag/AgCl reference electrode in H_2O at 289K temperature. Arrow describes origin and direction of scan.

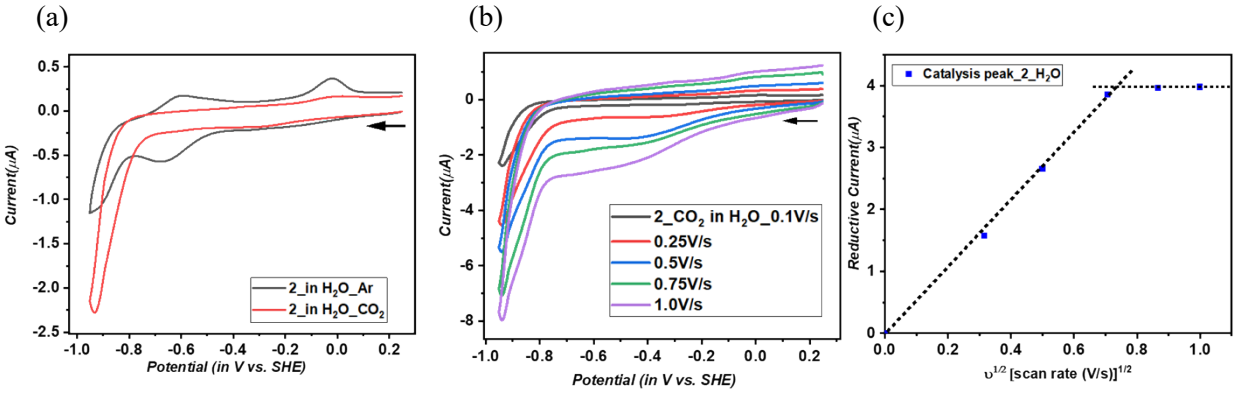

Figure S 24 CV studies of 2 under CO_2 in aqueous medium

Cyclic Voltammetry (CV) study in H_2O for complex 2; (a) CV spectra of 2 in H_2O under Ar (black trace) and CO_2 (red trace) atmospheres. (b) CV at different scan rate (0.1 V/sec to 1 V/sec) under CO_2; (b) $v^{1/2}$ vs reductive current plots of catalytic peak (-0.81 V). A 1mM catalyst in 0.1 M $KHCO_3$ was used with glassy carbon working electrode, Pt counter electrode, and Ag/AgCl reference electrode in H_2O at 289K temperature. Arrow describes origin and direction of scan. The potentials are reported vs SHE.

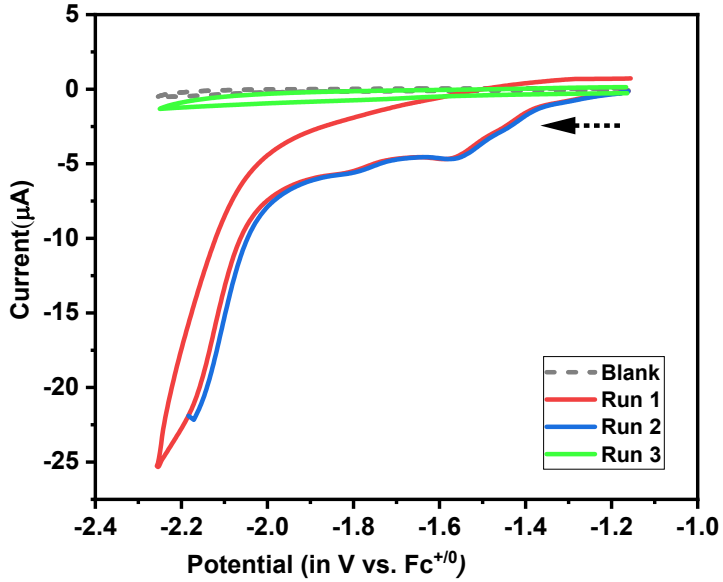

Figure S 25 Rinse test for 2

Rinse test experiment for 2 in DMF media. Initially a complete cyclic voltammogram (Run 1) was recorded under saturated CO_2 atmosphere. Then working electrode was thoroughly rinsed with water followed by through polishing with 0.25 μm alumina and another round of washing. Next, Run 2 was executed on the same solution by starting the scan form the same initial position as Run 1; however, it was stopped at the potential where the maximum catalytic response was noticed. Then the working electrode was only rinsed (no polishing) with water. This electrode was then included in a blank solution (that replicates the sample solution in all aspects other than the presence of the complex) and another voltammogram was recorded (Run 3) while starting from the potential where the maximum current position (catalytic CO_2 reduction) was observed. The horizontal arrows indicate the respective scan directions for each run. A 1mM catalyst in 0.1 M TBAF was used with glassy carbon working electrode, Pt counter electrode, and Ag/AgCl reference electrode at 289 K temperature at 0.1 V/sec scan rate.

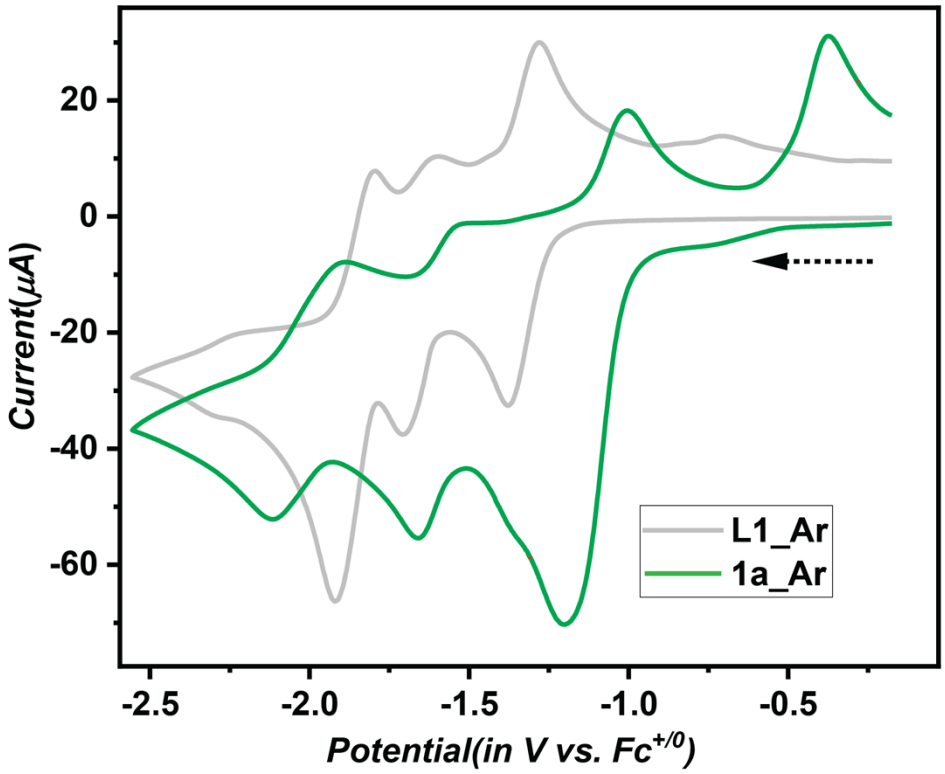

Figure S 26 CV studies of L1 and 1a under Ar

Comparative CV spectra for complex 1a (green trace) and ligand L1 (grey trace). A 1mM catalyst in 0.1 M TBAF was used with glassy carbon working electrode, Pt counter electrode, and Ag/AgCl reference electrode in DMF at 289K temperature at 0.1 V/sec. Arrow describes origin and direction of scan.

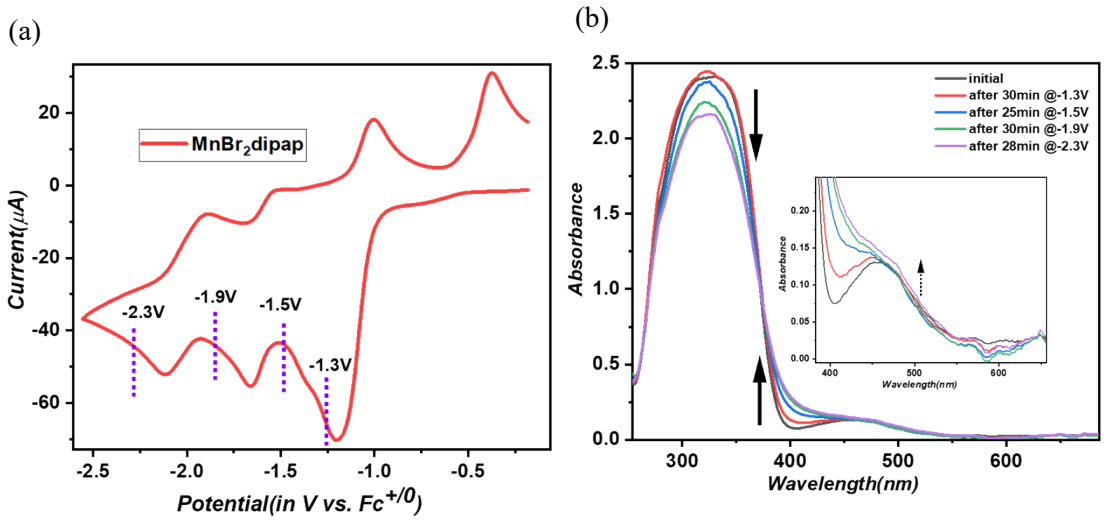

Figure S 27 UV-SEC analysis of 1a under Ar

(a) CV spectra of 1a under Ar in DMF highlighting the potentials that were held constant during UV-SEC studies. A 1mM catalyst in 0.1 M TBAF was used with glassy carbon working electrode, Pt counter electrode, and Ag/AgCl reference electrode in DMF at 289K temperature at 0.1 V/sec. (b) UV-sec studies showing changes in MLCT band. The inset highlights the changes between 400-650 nm.

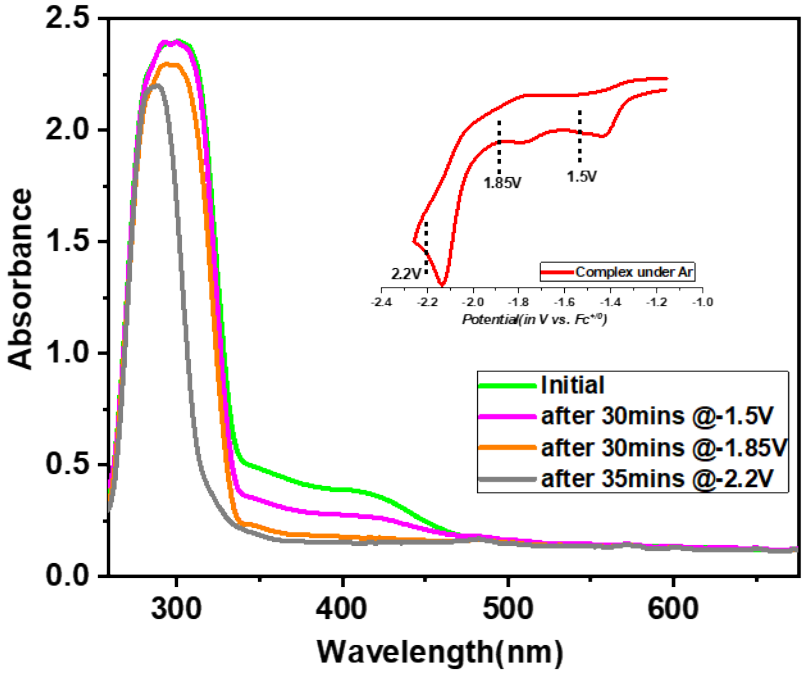

Figure S 28 UV-SEC studies of 2 in DMF under Ar

Optical spectra of 2 when no external potentials are applied (green trace). Changes in optical spectra when potentials were held constant at -1.5 V (pink trace), -1.85 V (orange trace), and -2.2 V (grey trace). Inset shows the CV spectra of 2 to highlight the various potentials held constant during SEC studies. The data were recorded under Ar at 298 K in DMF.

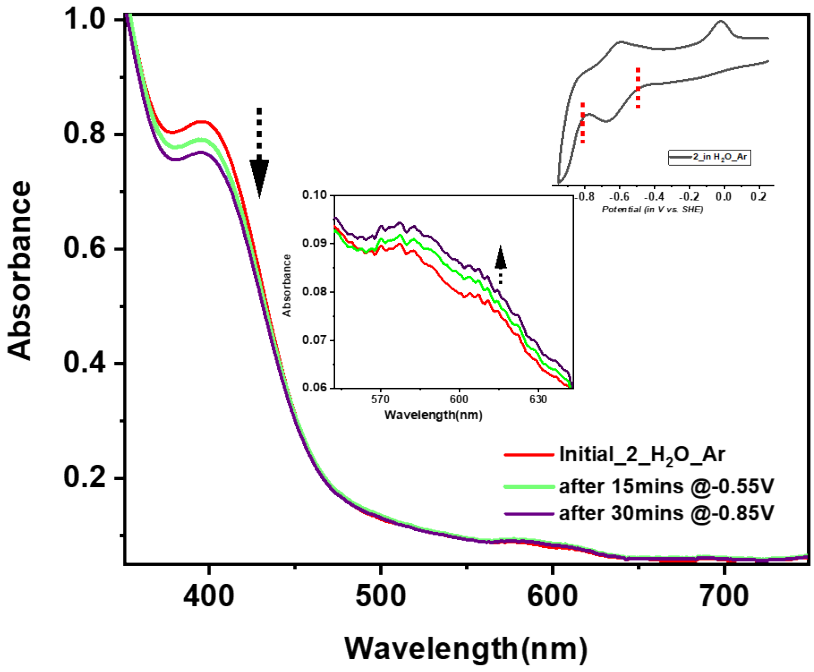

Figure S 29 UV-SEC studies of 2 in aqueous medium under Ar

Optical spectra of 2 when no external potentials are applied (red trace). Changes in optical spectra when potentials were held constant at -0.55 V (pink trace), and -0.85 V (orange trace). Insets show the changes in UV spectra between 550-650 nm range and the CV spectra of 2 in water to highlight the various potentials held constant during SEC studies. The data were recorded under Ar at 298 K in H_2O.

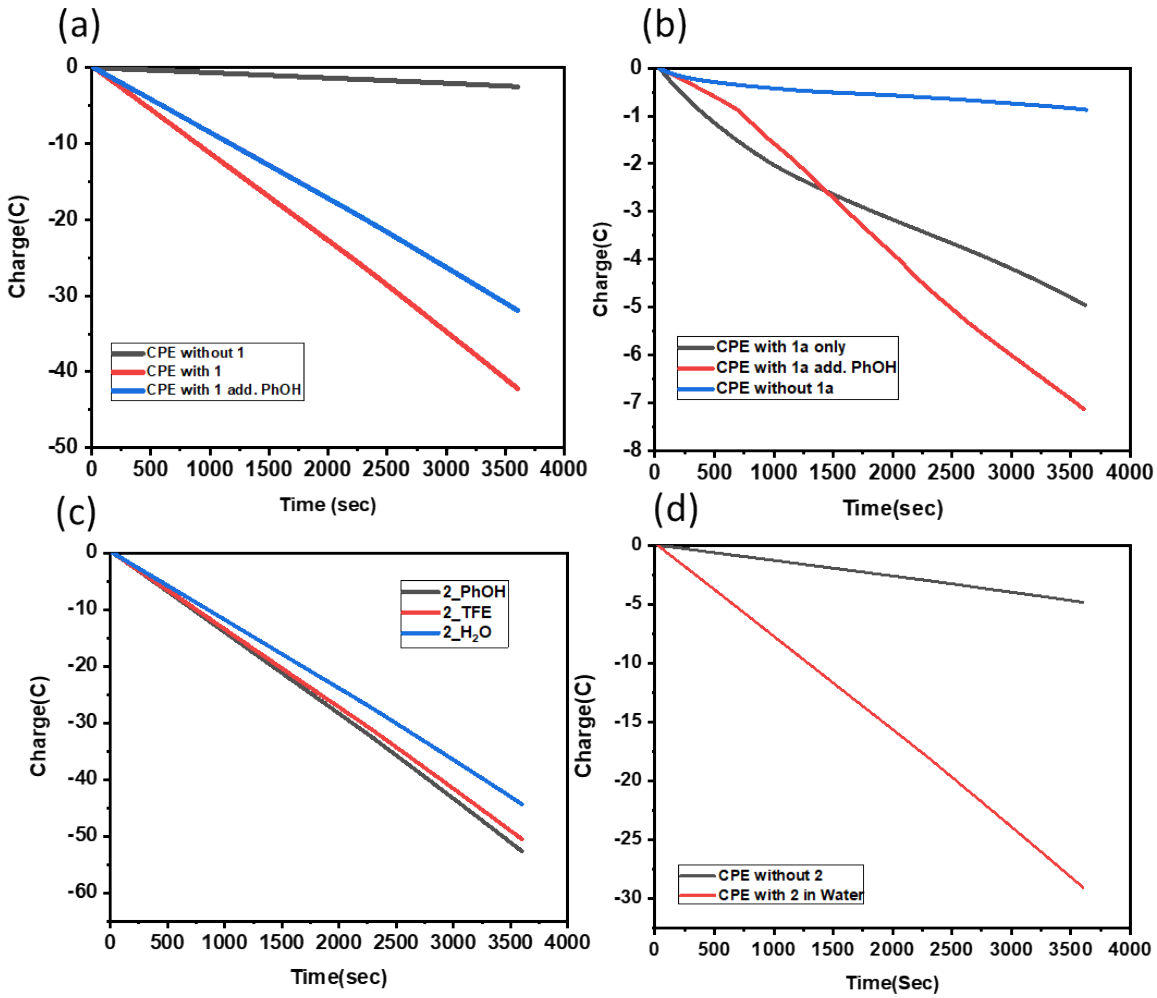

Figure S 30 Charge passed during Controlled Potential Electrolysis (CPE) study

Charge Passed during CPE in DMF of (a) 1 (red trace) and after adding PhOH (blue trace), (b) 1a (black trace) and after adding PhOH (red trace), (c) 2 in presence of PhOH (black trace), TFE(red trace) and H_2O (blue trace). (d) 2 in H_2O (red trace), without 2 (black trace).

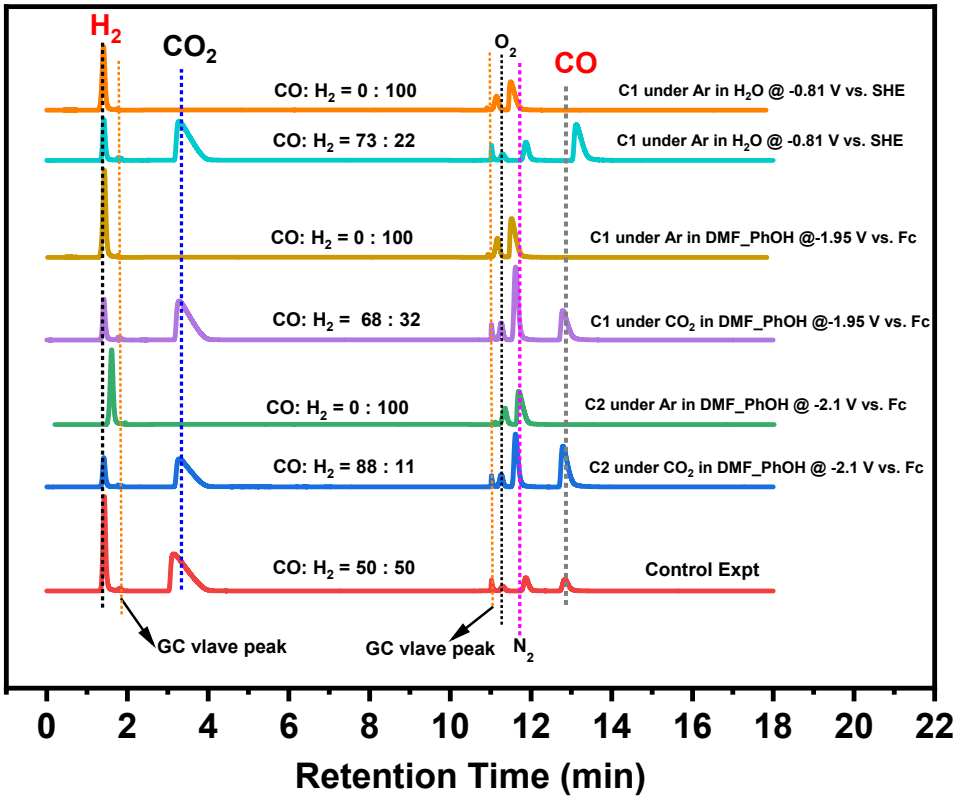

Figure S 31 GC analysis data during CPE

Gas Chromatography (GC) data recorded after injecting 0.5 mL of head space gas in the GC instrument using leur-lock gas-tight syringe after 3500 sec. Red trace is for standard 1:1 mixture of CO and H_2 gas from canister in absence of catalyst. Blue trace-**2** under CO_2 in water added DMF, green trace- **2** under Ar in water added DMF, purple trace- **1** under CO_2 in PhOH added DMF, amber trace- **1** under Ar in PhOH added DMF, cyan trace- **2** under CO_2 in H_2O, orange trace- **2** under Ar in H_2O.

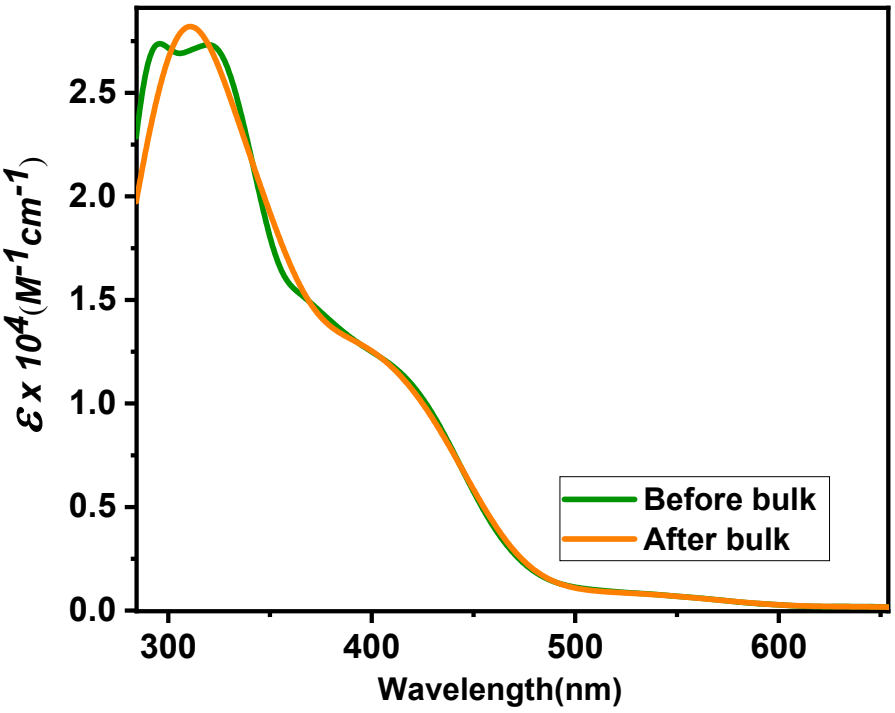

Figure S 32 Stability test for 2 before and after bulk analysis monitored by UV-Vis

Comparative optical spectra of 2, before (green trace) and after (orange trace) bulk analysis to understand the stability of the catalyst. All the spectra were recorded at room temperature scanning in the 250-800 nm range in DMF.

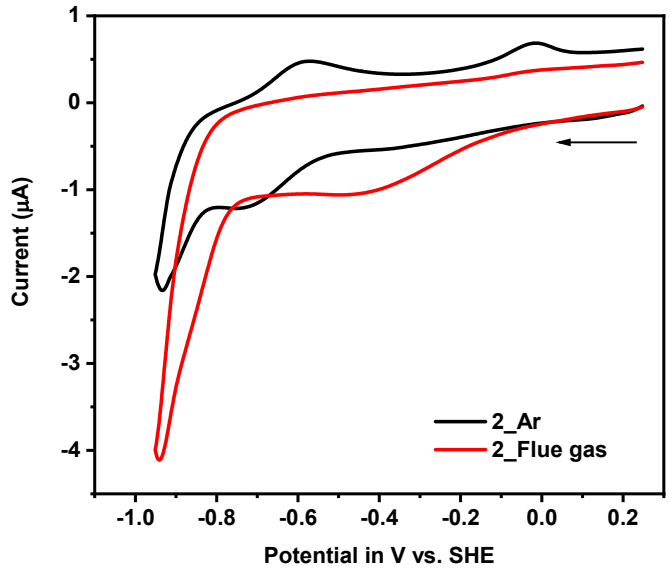

Figure S 33 CV studies of 2 under flue gas.

Comparative CV spectra for complex 2 under Ar (black trace) and in the presence of flue gas (red trace). A 1mM catalyst in 0.1 M $KHCO_3$ was used with glassy carbon working electrode, Pt counter electrode, and Ag/AgCl reference electrode in H_2O at 289K temperature at 0.1 V/sec. Arrow describes origin and direction of scan.

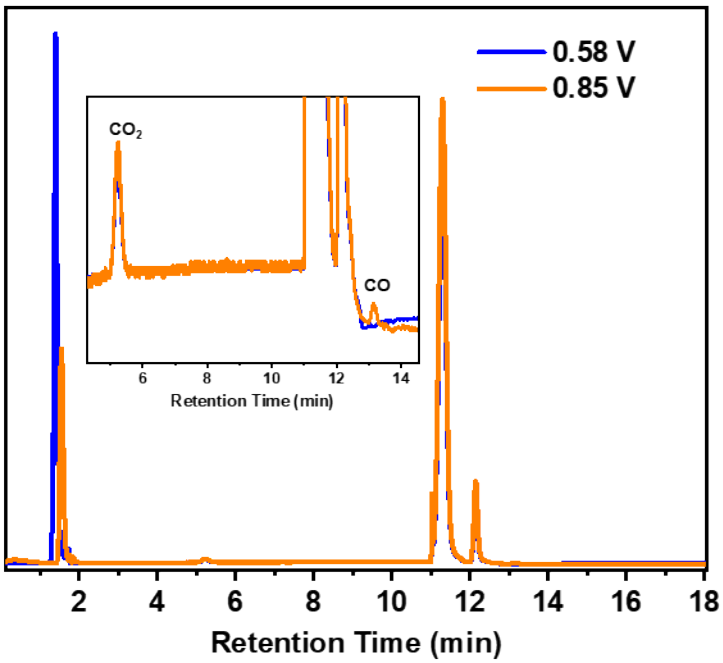

Figure S 34 GC analysis of 2 during CPE under flue gas in water.

Gas Chromatography (GC) data recorded after injecting 0.5 mL of head space gas in the GC instrument using leur-lock gas-tight syringe after 3500 sec at applied potentials of -0.58 V (blue trace) and -0.85 V (orange trace). Inset highlights the region from 6-14 min to observe the CO formation at retention time of 13.1 min.

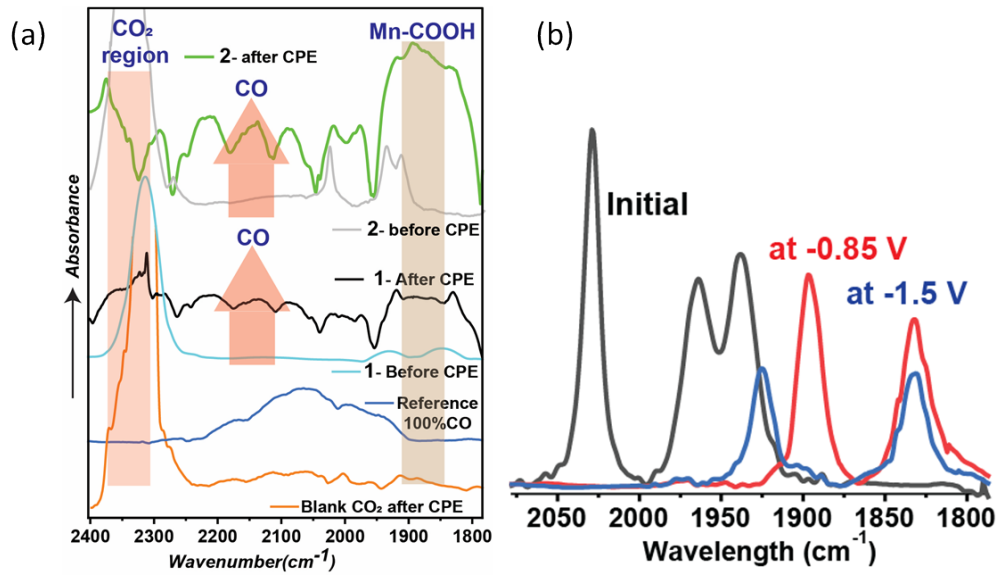

Figure S 35 IR-SEC of 1 and 2 under CO_2 in DMF

(**a**) IR spectra of solution without catalyst under CO_2 after CPE (orange trace), under CO (blue trace). Changes in the IR-SEC of **1** before (cyan trace) and after CPE (black trace). The changes in IR spectra of **1** was recorded at -1.95 V for 30 minutes. Changes in the IR-SEC of **2** before (grey trace) and after CPE (green trace).[12] The changes in IR spectra of **2** were documented at -2.2 V for 30 minutes. The vertical arrows indicate the changes of particular IR bands. (**b**) Alterations in CO stretching frequency of **1** pre-electrocatalysis (black trace), at -0.85 V (red trace), and -1.5 V (blue trace).

Table S 1 Crystal data and structure refinement for 1.

Identification code	2063724
Empirical formula	$C_{20}H_{13}BrMnN_5O_3$
Formula weight	506.20
Temperature/K	150.00(10)
Crystal system	triclinic
Space group	P-1
a/Å	7.9986(2)
b/Å	11.2283(5)
c/Å	12.0453(6)
α/°	75.135(4)
β/°	71.203(4)
γ/°	79.420(3)
Volume/Å^3	983.78(8)
Z	2
ρ_{calc}g/cm^3	1.709
μ/mm^{-1}	2.735
F(000)	504.0
Crystal size/mm^3	0.02 × 0.012 × 0.01
Radiation	MoKα (λ = 0.71073)
2Θ range for data collection/°	3.654 to 67.718
Index ranges	-11 ≤ h ≤ 12, -17 ≤ k ≤ 17, -18 ≤ l ≤ 18
Reflections collected	46525
Independent reflections	7006 [R_{int} = 0.1143, R_{sigma} = 0.1318]
Data/restraints/parameters	7006/0/271
Goodness-of-fit on F^2	1.035
Final R indexes [I>=2σ (I)]	R_1 = 0.0546, wR_2 = 0.0817
Final R indexes [all data]	R_1 = 0.1432, wR_2 = 0.1003
Largest diff. peak/hole / e Å^{-3}	0.63/-0.70

Table S 1a Important Bond Lengths for 1.

Atom	Atom	Length/Å
Mn1	Br1	2.5198(5)
Mn1	N1	1.975(2)
Mn1	N3	2.042(2)
Mn1	C1	1.808(3)
Mn1	C2	1.813(3)
Mn1	C3	1.842(3)
O1	C1	1.144(3)
O2	C2	1.122(4)
O3	C3	1.143(3)
N1	N2	1.272(3)
N4	N5	1.260(3)

Table S 2 Crystal data and structure refinement for 1a.

Identification code	2060736
Empirical formula	$C_{17}H_{13}Br_2MnN_5$
Formula weight	502.08
Temperature/K	150
Crystal system	orthorhombic
Space group	Pbca
a/Å	13.5517(9)
b/Å	15.3175(8)
c/Å	17.3668(12)
α/°	90
β/°	90
γ/°	90
Volume/Å^3	3605.0(4)
Z	8
ρ_{calc}g/cm^3	1.850
μ/mm^{-1}	5.175
F(000)	1960.0
Crystal size/mm^3	0.212 × 0.126 × 0.086
Radiation	MoKα (λ = 0.71073)
2Θ range for data collection/°	4.648 to 67.434
Index ranges	-18 ≤ h ≤ 20, -15 ≤ k ≤ 22, -23 ≤ l ≤ 19
Reflections collected	26572
Independent reflections	6094 [R_{int} = 0.1509, R_{sigma} = 0.1963]
Data/restraints/parameters	6094/0/226
Goodness-of-fit on F^2	0.875
Final R indexes [I>=2σ (I)]	R_1 = 0.0679, wR_2 = 0.1411
Final R indexes [all data]	R_1 = 0.2019, wR_2 = 0.2017
Largest diff. peak/hole / e Å^{-3}	0.76/-0.86

Table S 2a Important Bond Lengths for 1a

Atom	Atom	Length/Å
Mn1	Br2	2.4497(11)
Mn1	Br1	2.4467(12)
Mn1	N3	2.141(5)
Mn1	N5	2.393(5)
Mn1	N1	2.363(5)
N1	N2	1.264(7)
N4	N5	1.254(7)

Table S 3 Crystal data and structure refinement for 2.

Identification code	2236211
Empirical formula	$C_{15}BrMnN_6O_3$
Formula weight	447.06
Temperature/K	104.00(10)
Crystal system	orthorhombic
Space group	$Pca2_1$
a/Å	50.2984(12)
b/Å	6.8837(2)
c/Å	9.6648(3)
α/°	90
β/°	90
γ/°	90
Volume/Å^3	3346.33(16)
Z	8
ρ_{calc}g/cm^3	1.775
μ/mm^{-1}	3.205
F(000)	1728.0
Crystal size/mm^3	0.18 × 0.15 × 0.11
Radiation	Mo Kα (λ = 0.71073)
2Θ range for data collection/°	3.238 to 66.256
Index ranges	-75 ≤ h ≤ 75, -10 ≤ k ≤ 10, -14 ≤ l ≤ 14
Reflections collected	81284
Independent reflections	11714 [R_{int} = 0.1410, R_{sigma} = 0.1385]
Data/restraints/parameters	11714/1/209
Goodness-of-fit on F^2	2.017
Final R indexes [I>=2σ (I)]	R_1 = 0.1739, wR_2 = 0.3836
Final R indexes [all data]	R_1 = 0.2535, wR_2 = 0.4032
Largest diff. peak/hole / e Å^{-3}	9.32/-2.19
Flack parameter	0.331(17)

Table S 3a Important Bond Lengths for 2.

Atom	Atom	Length/Å
Mn1	Br1	2.540(3)
Mn1	N1	2.133(18)
Mn1	N2	2.090(18)
Mn1	C1	1.794(19)
Mn1	C3	1.73(2)
Mn1	C2	1.79(2)
O1	C1	1.08(2)
O2	C2	1.26(3)
O3	C3	1.17(3)

Table S 4 Comparative data of bond lengths and IR stretching frequencies of complexes 1 and 2

Bond Parameters and IR stretching	Complex 1	Complex 2
$Mn\text{-}N_{Pyr}$	2.042 Å	2.132 Å
$Mn\text{-}N_{Azo}$	1.975 Å	-
$Mn\text{-}N_{Tria}$	-	2.092 Å
Mn-Br	2.520 Å	2.540 Å
$Mn\text{-}CO_{trans\ to\ Br}$	1.813 Å	1.794 Å
$Mn\text{-}CO_{trans\ to\ N\_Pyr}$	1.808 Å	1.734 Å
$Mn\text{-}CO_{trans\ to\ N\_Azo}$	1.842 Å	-
$Mn\text{-}CO_{trans\ to\ N\_Tria}$	-	1.793 Å
$\nu_{CO(sym)}$	2028 cm^{-1}	2026 cm^{-1}
$\nu_{CO(asym)1}$	1963 cm^{-1}	1937 cm^{-1}
$\nu_{CO(asym)2}$	1938 cm^{-1}	1914 cm^{-1}

Abbreviations: Pyr = Pyridine, Tria = Triazole

Catalyst	Solvent	Gas	External proton source	Applied Potential (V)*	Overpotential (mV)	FE_{CO}	FE_{H_2}	TON in 1 h
1	DMF	CO_2	-	-1.95	140	75	11	121
		CO_2	PhOH	-1.95	140	73	16	117
				-1.90	90	70	26	98
1a	DMF	CO_2	-	-1.95	-	<1	28	-
		CO_2	PhOH	-1.95	-	<1	42	-
2	DMF	CO_2	-	-2.1	290	78	09	478
		CO_2	H_2O	-2.1	290	88	11	534
				-2.0	190	84	16	511
		CO_2	PhOH	-2.1	290	87	11	528
				-2.0	190	81	17	502
		CO_2	TFE	-2.1	290	86	11	524
				-2.0	190	80	18	496
	$KHCO_3$ aqueous buffer	CO_2	pH = 7.0	-0.81	270	73	22	113
	$KHCO_3$ aqueous buffer	Flue Gas **CO_2 (15 %)** NO_2(100 ppm) NO_2(500 ppm) O_2 (5 %) Balanced with N_2	pH = 7.9	-0.58	-	0	83	-
				-0.85	310	62	37	32

Table S 5 Electrochemical parameters for catalysts in DMF and water

*Applied potentials values are reported vs. ferrocenium/ferrocene couple in DMF except for the last 2 entries in aqueous solution where potential is reported vs. SHE.

References:

(1) Chowdhury, A. D.; Das, A.; K, I.; Mobin, S. M.; Lahiri, G. K. Isomeric Complexes of [RuII(Trpy)(L)Cl] (Trpy = 2,2′:6′,2″-Terpyridine and HL = Quinaldic Acid): Preference of Isomeric Structural Form in Catalytic Chemoselective Epoxidation Process. *Inorg. Chem.* **2011**, *50* (5), 1775–1785. https://doi.org/10.1021/ic102195w.

(2) Bentiss, F.; Lagrenée, M.; Barbry, D. Accelerated Synthesis of 3,5-Disubstituted 4-Amino-1,2,4-Triazoles under Microwave Irradiation. *Tetrahedron Letters* **2000**, *41* (10), 1539–1541. https://doi.org/10.1016/S0040-4039(99)02350-3.

(3) Shen, J.; Li, H. An Empirical Analysis on Industrial Organization Structure of Chinese Software Service Outsourcing. *JSSM* **2010**, *03* (02), 218–226. https://doi.org/10.4236/jssm.2010.32027.

(4) Sheldrick, G. M. Crystal Structure Refinement with SHELXL. *Acta Cryst C* **2015**, *71* (1), 3–8. https://doi.org/10.1107/S2053229614024218.

(5) Dolomanov, O. V.; Bourhis, L. J.; Gildea, R. J.; Howard, J. a. K.; Puschmann, H. OLEX2: A Complete Structure Solution, Refinement and Analysis Program. *J Appl Cryst* **2009**, *42* (2), 339–341. https://doi.org/10.1107/S0021889808042726.

(6) Sheldrick, G. M. A Short History of SHELX. *Acta Crystallogr A* **2008**, *64* (Pt 1), 112–122. https://doi.org/10.1107/S0108767307043930.

(7) Macrae, C. F.; Sovago, I.; Cottrell, S. J.; Galek, P. T. A.; McCabe, P.; Pidcock, E.; Platings, M.; Shields, G. P.; Stevens, J. S.; Towler, M.; Wood, P. A. Mercury 4.0: From Visualization to Analysis, Design and Prediction. *J Appl Cryst* **2020**, *53* (1), 226–235. https://doi.org/10.1107/S1600576719014092.

(8) Westrip, S. P. publCIF: Software for Editing, Validating and Formatting Crystallographic Information Files. *J Appl Cryst* **2010**, *43* (4), 920–925. https://doi.org/10.1107/S0021889810022120.

(9) Carlos, R. M.; Neumann, M. G. Photochemical and Photophysical Properties of [Mn(Imidazole)(CO)3(Phen)](SO3CF3) Complexes. *Journal of Photochemistry and Photobiology A: Chemistry* **2000**, *131* (1), 67–73. https://doi.org/10.1016/S1010-6030(99)00241-5.

(10) Tamer, Ö. A Unique Manganese (II) Complex of 4-Methoxy-Pyridine-2-Carboxylate: Synthesis, Crystal Structure, FT-IR and UV–Vis Spectra and DFT Calculations. *Journal of Molecular Structure* **2017**, *1144*, 370–378.

(11) Biswas, S.; Mitra, K.; Chattopadhyay, S. K.; Adhikary, B.; Lucas, C. Robert. Mononuclear Manganese(II) and Manganese(III) Complexes of N2O Donors Involving Amine and Phenolate Ligands: Absorption Spectra, Electrochemistry and Crystal Structure of [Mn(L3)2](ClO4). *Transition Metal Chemistry* **2005**, *30* (4), 393–398. https://doi.org/10.1007/s11243-004-7542-6.

(12) Wang, J.-W.; Luo, Z.-M.; Yang, G.; Gil-Sepulcre, M.; Kupfer, S.; Rüdiger, O.; Ouyang, G. Highly Efficient Electrocatalytic CO2 Reduction by a CrIII Quaterpyridine Complex. *Proceedings of the National Academy of Sciences* **2024**, *121* (14), e2319288121.